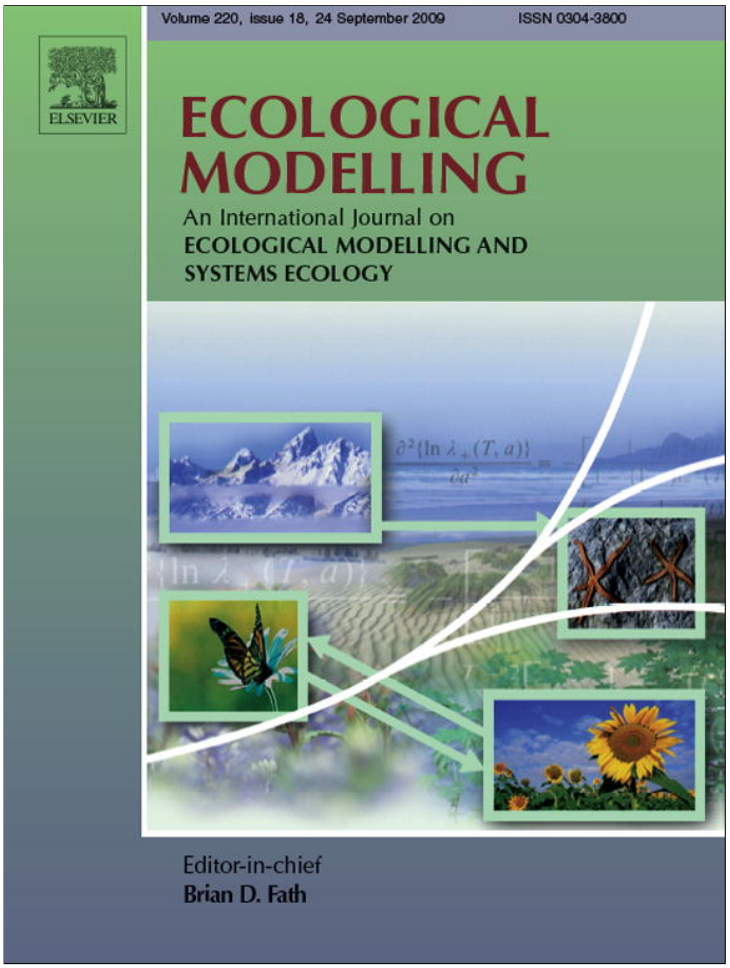

Ecological Modelling 220 (2009) 2142–2161

Contents lists available at ScienceDirect

Ecological Modelling

journal homepage: www.elsevier.com/locate/ecolmodel

A Bayesian hierarchical framework for calibrating aquatic biogeochemical models

Weitao Zhang[a], George B. Arhonditsis[a,b,*]

[a] Department of Geography, University of Toronto, Toronto, Ontario, Canada, M5S 3G3
[b] Department of Physical & Environmental Sciences, University of Toronto, Toronto, Ontario, Canada, M1C 1A4

ARTICLE INFO

Article history:
Received 15 September 2008
Received in revised form 20 May 2009
Accepted 29 May 2009
Available online 3 July 2009

Keywords:
Bayesian calibration
Eutrophication
Uncertainty analysis
Aquatic biogeochemical models
Hierarchical Bayes
Mathematical modeling

ABSTRACT

Model practitioners increasingly place emphasis on rigorous quantitative error analysis in aquatic biogeochemical models and the existing initiatives range from the development of alternative metrics for goodness of fit, to data assimilation into operational models, to parameter estimation techniques. However, the treatment of error in many of these efforts is arguably selective and/or ad hoc. A Bayesian hierarchical framework enables the development of robust probabilistic analysis of error and uncertainty in model predictions by explicitly accommodating measurement error, parameter uncertainty, and model structure imperfection. This paper presents a Bayesian hierarchical formulation for simultaneously calibrating aquatic biogeochemical models at multiple systems (or sites of the same system) with differences in their trophic conditions, prior precisions of model parameters, available information, measurement error or inter-annual variability. Our statistical formulation also explicitly considers the uncertainty in model inputs (model parameters, initial conditions), the analytical/sampling error associated with the field data, and the discrepancy between model structure and the natural system dynamics (e.g., missing key ecological processes, erroneous formulations, misspecified forcing functions). The comparison between observations and posterior predictive monthly distributions indicates that the plankton models calibrated under the Bayesian hierarchical scheme provided accurate system representations for all the scenarios examined. Our results also suggest that the Bayesian hierarchical approach allows overcoming problems of insufficient local data by "borrowing strength" from well-studied sites and this feature will be highly relevant to conservation practices of regions with a high number of freshwater resources for which complete data could never be practically collected. Finally, we discuss the prospect of extending this framework to spatially explicit biogeochemical models (e.g., more effectively connect inshore with offshore areas) along with the benefits for environmental management, such as the optimization of the sampling design of monitoring programs and the alignment with the policy practice of adaptive management.

1. Introduction

Many freshwater ecosystems are currently jeopardized by human intrusion, without proper documentation of their baseline state and how humans have altered their biotic communities and biogeochemical cycles. The invasion of biotic communities by non-native species is perhaps the greatest threat to the integrity of lakes and rivers (Schindler, 2001). Climate-induced chemical and biological responses in lakes are another important issue, and several ecological and biogeochemical studies have shown a coupling among lake temperatures and water chemistry, individual organism physiology, population abundance, and community structure (Schindler, 1997; Straile, 2002; Weyhenmeyer, 2004). Climate forcing can have different effects on various taxonomic groups/trophic levels, and decouple species from favorable food conditions with dire consequences on ecosystem functioning (Thomas et al., 2001; Hampton, 2005). Therefore, the development of holistic understanding of the climate-driven aquatic ecosystem responses requires consideration of the complex interplay between physical, chemical factors and multiple trophic levels at a variety of spatial and temporal scales. Given the increasingly ominous context, the demand for reliable modeling tools that can offer insights into the ecosystem dynamics and effectively support environmental management is more pressing than ever before (Arhonditsis and Brett, 2004; Arhonditsis et al., 2006). However, the general lack of uncertainty estimates for most environmental models, the arbitrary selection of higher, more costly, and often unattainable threshold values for environmental variables as a hedge against unknown

* Corresponding author at: Department of Physical & Environmental Sciences, University of Toronto, Toronto, Ontario, Canada, M1C 1A4. Tel.: +1 416 208 4858; fax: +1 416 287 7279.
E-mail address: georgea@utsc.utoronto.ca (G.B. Arhonditsis).

0304-3800/$ – see front matter © 2009 Elsevier B.V. All rights reserved.
doi:10.1016/j.ecolmodel.2009.05.023

prediction errors, risky model-based management decisions and unanticipated system responses are often experienced in the current management practice.

Uncertainty analysis of mathematical models has been a central topic in aquatic ecosystem research, and there have been several attempts to rigorously assess model error associated with model structure and parameter uncertainty (Omlin and Reichert, 1999; Brun et al., 2001; Reichert et al., 2002; Chen et al., 2007). Model uncertainty analysis essentially aims to make inference about the joint probability distribution of model inputs, reflecting the amount of knowledge available for model parameters, initial conditions, forcing functions, and model structure. In this regard, Bayes' Theorem provides a convenient means to combine existing information (prior) with current observations (likelihood) for projecting future ecosystem response (posterior). Hence, the Bayesian techniques are more informative than the conventional model calibration practices (i.e., mere adjustment of model parameters until the discrepancy between model outputs and observed data is minimized), and can be used to refine our knowledge of model input parameters while obtaining predictions along with uncertainty bounds for output variables (Arhonditsis et al., 2007). Nonetheless, despite the compelling arguments for considering Bayesian inference techniques as an integral part of the model development process, their high computational demands along with the lack of analytical expressions for the posterior distributions was until recently a major impediment for their broader application (Reichert and Omlin, 1997).

Elucidation of the uncertainty patterns in the multidimensional parameter spaces of mathematical models involves two critical steps: (i) selection of the likelihood function to quantify model misfit, and (ii) selection of the sampling scheme for generating input vectors which then are evaluated with regards to the model performance. The latter decision addresses the sampling efficiency of the approach, e.g., Random sampling, Latin hypercube, Markov chain Monte Carlo (MCMC). Many Bayesian or non-Bayesian uncertainty analysis applications (e.g., Generalized Likelihood Uncertainty Estimation, Bayesian Monte Carlo) have been combined with sampling algorithms which draw samples uniformly and independently from the prior parameter space. These strategies often result in Monte Carlo samples that misrepresent (or insufficiently cover) regions of high model likelihood; especially, when the joint prior parameter distribution is very wide or the parameters are highly correlated (Qian et al., 2003). To address this problem, several recent studies advocate the use of MCMC sampling schemes that are specifically designed to sample directly from the posterior distribution and to converge to the higher model likelihood regions (Gelman et al., 1995; Arhonditsis et al., 2007; Stow et al., 2007). On the other hand, the selection of the model likelihood function entails conceptual dilemmas involving the selection of generalized (e.g., root mean square error, reliability index, *U*-uncertainty) or purely probabilistic (e.g., normal, lognormal or Poisson error) likelihood functions that can significantly alter the results (Beven, 2001). In typical uncertainty analysis applications, the likelihood function is broadly specified as any measure of goodness of-fit that can be used to compare observed data with model predictions, e.g., sum of squared errors, fuzzy measures or even qualitative measures for model evaluation (Franks et al., 1998; Beven, 2001; Page et al., 2004). However, it has been argued that unless the likelihood function corresponds to a formal probability distribution that directly connects the data with model input parameters and output state variables, the uncertainty analysis results do not have a clear Bayesian interpretation (Engeland and Gottschalk, 2002; Hong et al., 2005).

In the context of water quality modeling, there are several recent studies illustrating how the Bayesian inference techniques combined with MCMC sampling schemes can improve model forecasts and management actions over space and time. For example, Malve et al. (2005) showed how the Bayesian parameter estimation of a dynamic non-linear model can be used to quantify the winter respiration rates (oxygen depletion per unit area of hypolimnetic surface) in a hyper-eutrophic shallow Finnish lake. A conceptually similar modeling approach was also used to elucidate the confounded bottom-up and top-down effects on the phytoplankton community structure of the shallow, mesotrophic Lake Pyhäjärvi (Malve et al., 2007). Arhonditsis et al. (2007, 2008a) introduced a Bayesian calibration scheme using simple mathematical models (<10 state variables) and statistical formulations that explicitly accommodate measurement error, parameter uncertainty, and model structure error; this framework was then used to quantify the information the data contain about model inputs, to offer insights into the covariance structure among parameter estimates, and to obtain predictions along with credible intervals for model outputs. A follow-up study examined the efficiency of two uncertainty analysis strategies, a typical Generalized Likelihood Uncertainty Estimation (GLUE) approach combined with a random sampling scheme vis-á-vis a formal probabilistic model configuration updated with MCMC simulations, to elucidate the propagation of uncertainty through the input spaces of simple numerical aquatic biogeochemical models (Arhonditsis et al., 2008b). Finally, a recent study integrated the Bayesian calibration framework with a complex aquatic biogeochemical model simulating multiple elemental cycles and functional plankton groups to illustrate how the Bayesian parameter estimation can be used for assessing the exceedance frequency and confidence of compliance of different water quality criteria (Zhang and Arhonditsis, 2008).

In this paper, we present another prospect of the Bayesian inference techniques by introducing a hierarchical formulation for calibrating aquatic biogeochemical models at multiple sites. This illustration is based on several synthetic datasets representing oligo-, meso- and eutrophic lake conditions. Our objective is to examine if the incorporation of mathematical models into Bayesian hierarchical frameworks can assist the effective modeling of systems with limited information by enabling the transfer of information across systems. With the hierarchical model configuration, we can potentially overcome problems of insufficient local data by "borrowing strength" from well-studied sites on the basis of distributions that connect systems in space. This outcome is highly relevant to conservation practices of regions with a high number of freshwater resources for which complete data could never be practically gathered. Finally, we discuss the prospect of extending this framework to coupled physical-biogeochemical models along with its benefits to environmental management, such as the optimization of the sampling design of monitoring programs and the alignment with the policy practice of adaptive management.

2. Methods

Hierarchical Bayes allows decomposing the environmental problems into intuitively manageable levels, thereby offering a conceptually plausible means for addressing the complexity pervading the natural systems (Clark, 2005). As such, the Bayesian hierarchical modeling can be an indispensable methodological framework to disentangle complex ecological patterns, to exploit disparate sources of ecological information, to accommodate tightly intertwined environmental processes operating at different spatiotemporal scales, and to explicitly consider the variability pertaining to latent variables or other inherently unmeasurable quantities (Wikle, 2003a; Clark, 2005). Furthermore, Wikle (2003a) argued that rather than specifying the ecological dynamics as joint multivariate spatiotemporal covariance structures, it would also be statistically easier to factor such joint distributions into a series of conditional models, i.e., dissect the total process into a number of connected subprocesses. The essence of the Bayesian hierarchical

thinking is that the environmental complexity can be decomposed into the following series of models coherently linked together via Bayes' rule (Berliner, 1996):

$$\underbrace{[\text{process, parameters}|\text{data}]}_{\text{Posterior distribution}} \propto \underbrace{[\text{data}|\text{process, parameters}]}_{\text{Data model}} \times \underbrace{[\text{process}|\text{parameters}]}_{\text{Process model}} \times \underbrace{[\text{parameters}]}_{\text{Parameter model}} \quad (1)$$

where the posterior distribution reflects our beliefs on the levels of the process and parameters after the data updating, which can be thought of as the product of the data model, specifying the dependence of the observed data on the process of interest and parameters, with the process model, describing the process conditional on other parameters, and the parameter model, quantifying the uncertainty in parameter values. Each of these models may then consist of multiple substages to account for the role of an inconceivably complex array of environmental functions that comes into play in real world applications (Wikle, 2003a).

In environmental science, the general formula (1) has been used to predict demographic processes and spatiotemporal population spread (Wikle, 2003b; Clark, 2005), to incorporate physically based prior information on simulated geophysical processes (Royle et al., 1999; Wikle et al., 2001), to stochastically treat boundary conditions in coupled atmospheric–ocean models (Wikle et al., 2003), and more recently to resolve the mechanisms of species coexistence and the biodiversity paradox (Clark et al., 2007). The present study extends the application of Bayesian hierarchical structures with process-based models, and our aim is (i) to illustrate how they can assist in sharing information among different systems (or sites); and (ii) to obtain predictions along with uncertainty bounds that take into account the insufficient amount of information in less studied systems as well as the variability observed across systems.

2.1. Bayesian hierarchical framework

Our statistical formulation explicitly considers the uncertainty in model inputs (model parameters, initial conditions), the analytical/sampling error associated with the field data, and the discrepancy between model structure and the natural system dynamics (e.g., missing key ecological processes, erroneous formulations, misspecified forcing functions). Earlier applications of this formulation have resulted in an improvement of the model performance, i.e., the median predictions along with the 95% credible intervals delineate zones that accurately describe the observed data (Arhonditsis et al., 2007, 2008a,b). In this study, the Bayesian hierarchical framework builds upon the assumption that the model discrepancy is invariant with the input conditions, and thus the difference between model and system dynamics is constant over the annual cycle for each state variable. The hierarchical structures examined consist of two submodels representing two local aquatic systems (or two sites of the same system) with differences in their trophic conditions, prior precisions of model parameters, available information, measurement error or inter-annual variability (Table 1). In particular, the first scenario considers a mesotrophic system combined with an oligotrophic or eutrophic one, aiming to examine the posterior patterns when crossing different trophic states under the hierarchical framework. Two mesotrophic datasets with different inter-annual variability (15% and 30%) were used in scenario *B*, thereby assessing the robustness of the results if, for example, we explicitly consider both dynamic (inshore) and static (offshore) areas of the same system during the model calibration process. The focus of the third scenario was to compare how the two submodels will be calibrated when combining systems (or sites) with different sampling intensity (C_1 and C_2) or systems with different dynamics, e.g., vertical mixing regimes (C_3). The scenario *D* extends the scheme examined in the scenario *A* by increasing the prior standard deviations of the system-specific parameters. This numerical experiment relaxes our confidence on the knowledge used to formulate the global priors and broadens the parameter space examined during the calibration of the two submodels. Based on these scenarios, the hierarchical modeling framework can be summarized as follows (Fig. 1a):

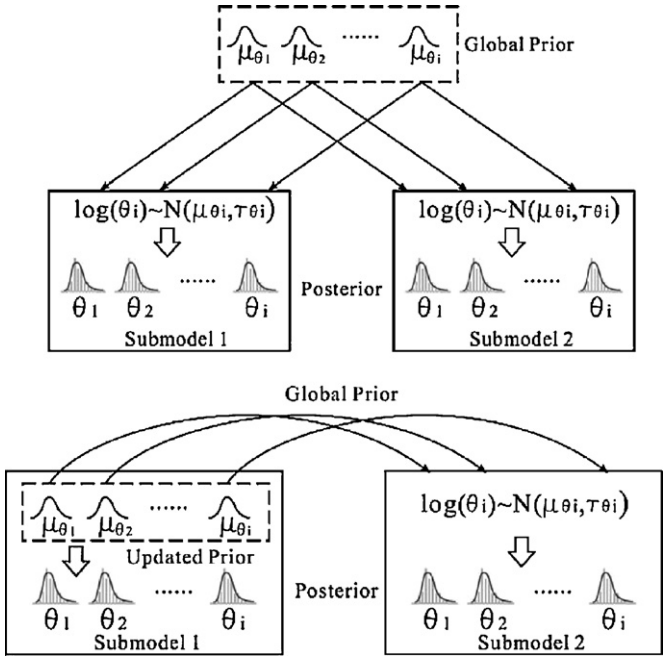

Fig. 1. The structure of the two hierarchical frameworks examined: (a) scenarios *A*, *B*, *C*, and *D*; (b) scenario *E*.

$$y_{ijk} \sim N(f(\theta_k, x_{ik}, y_{0k}), \sigma^2_{ijk}) \quad (2)$$

$$\theta_k \sim N(\theta, \tau^2_k) \quad y_{0k} \sim N(y_{1k}, k^2_k) \quad (3)$$

$$\log(\theta) \sim N(\mu, \tau^2) \quad (4)$$

$$\sigma^2_{ijk} = \delta^2_{jk} + \varepsilon^2_{ijk} \quad (5)$$

$$\delta^2_{jk} \sim \text{Inv-Gamma}(0.01, 0.01) \quad (6)$$

$$\tau^2_k = (\alpha_1 \times \theta)2; k^2_k = (\alpha_2 \times y_{ik})^2; \varepsilon^2_{ijk} = (\alpha_3 \times y_{ijk})^2$$
$$i = 1, \ldots, n; j = 1, \ldots, m; k = 1, \ldots, o \quad (7)$$

where y_{ijk} is the *i*th observed value of the *j*th state variable in the system (or site of the same system) *k*; $f(\theta_k, x_{ik}, y_{0k})$ is the numerical solution of the eutrophication model; x_{ik} is a vector of time dependent control variables (e.g., boundary conditions, forcing functions) describing the environmental conditions in the system (or site of the same system) *k*, the vector θ_k is a time independent set of the calibration model parameters (i.e., the 14 parameters in Table 2) derived from *k* system-specific normal distributions with means drawn from the global prior θ and standard deviations τ_k equal to α_1 (=15, 35)% of the corresponding mean values; μ, τ^2 represent the first and second order moments of the hyperparameter distributions; y_{0k} corresponds to the concentrations of the state variables at the initial time point t_0 derived from normal prior distributions with mean values the January monthly averages y_{1k} and standard deviation that was α_2 (=15)% of the mean value for each state variable *j*; δ_{jk} is a state variable and system-specific error term representing the discrepancy between the model structure and the natural system dynamics; ε_{ijk} is the measurement error associated

Table 1
The scenarios examined along with the general questions addressed under the Bayesian hierarchical configuration of the mathematical model.

Scenario no.	Submodel	Measurement error	Parameter precision	Inter-annual variability	Trophic state	Observed data availability
(A) How robust are the posterior patterns when combining sites of different trophic states (e.g., a eutrophic embayment with the central part of a lake)?						
	1	15%	15%	15%	Mesotrophic	12 monthly values
A_1	2	15%	15%	15%	Oligotrophic	12 monthly values
	1	15%	15%	15%	Mesotrophic	12 monthly values
A_2	2	15%	15%	15%	Eutrophic	12 monthly values
(B) How robust are the posterior patterns when combining sites of different inter-annual variability (e.g., inshore and offshore areas of the same system)?						
	1	15%	15%	15%	Mesotrophic	12 monthly values
B_1	2	15%	15%	30%	Mesotrophic	12 monthly values
(C) How robust are the posterior patterns when combining systems and/or sites with different sampling intensity (C_1 and C_2) or systems with different hydrodynamics (C_3)?						
	1	15%	15%	15%	Mesotrophic	12 monthly values
C_1	2	25%	15%	15%	Mesotrophic	4 seasonal values
	1	15%	15%	15%	Mesotrophic	12 monthly values
C_2	2	15%	15%	15%	Mesotrophic	6 monthly values during the stratified period
	1	15%	15%	15%	Mesotrophic	12 monthly values
C_3	2	15%	15%	15%	Eutrophic dimictic	6 monthly values during the ice-free period
(D) How robust are the posterior patterns when combining systems of different trophic states, and we are less confident on the knowledge used to formulate the global priors?						
	1	15%	35%	15%	Mesotrophic	12 monthly values
D_1	2	15%	35%	15%	Oligotrophic	12 monthly values
	1	15%	35%	15%	Mesotrophic	12 monthly values
D_2	2	15%	35%	15%	Eutrophic	12 monthly values
(E) How robust are the posterior patterns when combining a "refined" parameterization stemming from a well-studied system with a less intensively studied system?						
	1	15%	Updated prior	15%	Mesotrophic	12 monthly values
E_1	2	15%	15%	15%	Eutrophic	12 monthly values
	1	15%	Updated prior	15%	Mesotrophic	12 monthly values
E_2	2	25%	15%	15%	Mesotrophic	4 seasonal values

with each observation y_{ijk} assumed to be α_3 (=15, 25)% of the corresponding values; m, n, and o correspond to the number of state variables (m = 4), the number of observations in time used to calibrate the model (n = 4, 6, and 12 average monthly values), and the number of systems (or sites of the same system) incorporated into the hierarchical framework (o = 2), respectively.

We also examined if a "refined" parameterization stemming from a well-studied system can improve model performance in less intensively studied systems (scenario *E*). Namely, the system represented from the first submodel underwent a preliminary training (calibration) prior to the configuration of the hierarchical framework. The updated parameter distributions served as the global priors which then were used to delineate the two system-specific parameter spaces (Fig. 1b). The first submodel was subject to a second calibration exercise with a qualitatively similar dataset, whereas the second submodel was firstly tested against an eutrophic dataset (E_1) and subsequently against a system for which only four seasonal averages were available (E_2). Under the fifth scenario, the hierarchical framework can be summarized as follows:

$$y_{ijk} \sim N(f(\theta_k, x_{ik}, y_{0k}), \sigma^2_{ijk}) \quad (8)$$

$$\theta_k \sim N(\theta, \tau^2_k) \quad y_{0k} \sim N(y_{1k}, k^2_k) \quad (9)$$

$$\log(\theta) \sim N_l(\hat{\theta}, \Sigma) \quad (10)$$

$$\sigma^2_{ijk} = \delta^2_{jk} + \varepsilon^2_{ijk} \quad (11)$$

$$\delta^2_{j1} \sim \text{Inv-Gamma}(\alpha, \beta) \quad (12)$$

$$\delta^2_{j2} \sim \text{Inv-Gamma}(0.01, 0.01) \quad (13)$$

$$\tau^2_k = (\alpha_1 \times \theta)^2; k^2_k = (\alpha_2 \times y_{ik})^2; \varepsilon^2_{ijk} = (\alpha_3 \times y_{ijk})^2$$
$$i = 1, \ldots, n; j = 1, \ldots, 4; k = 1, 2; l = 14 \quad (14)$$

where θ represents the global prior drawn from a l-dimensional multivariate normal distribution with mean $\hat{\theta}$ and covariance matrix Σ derived from the original model calibration in the well-studied system; and α, β correspond to the shape and scale parameters of the updated j inverse-gamma distributions after the first model training.

Table 2
The prior probability distributions of the hyperparameters.

Parameter	Units	Mean	S.D.
Maximum phytoplankton growth rate (a)	day^{-1}	1.446	0.308
Zooplankton mortality rate (d)	day^{-1}	0.173	0.021
Half-saturation constant for predation (pred)	$mg\,C\,m^{-3}$	54.61	13.94
Half-saturation constant for PO_4 uptake (e)	$mg\,P\,m^{-3}$	10.93	4.818
Cross-thermocline exchange rate (k)	day^{-1}	0.037	0.013
Phytoplankton respiration rate (r)	day^{-1}	0.117	0.070
Phytoplankton sinking loss rate (s)	day^{-1}	0.040	0.032
Zooplankton growth efficiency (a)		0.366	0.126
Zooplankton excretion fraction (β)		0.293	0.111
Regeneration of zooplankton predation excretion (γ)		0.293	0.111
Maximum zooplankton grazing rate (λ)	day^{-1}	0.609	0.107
Zooplankton grazing half-saturation coefficient (μ)	$mg\,P\,m^{-3}$	6.575	1.867
Detritus remineralization rate (φ)	day^{-1}	0.092	0.032
Detritus sinking rate (ψ)	day^{-1}	0.142	0.084

2.2. Mathematical model

We used a zero-dimensional (single compartment) model that considers the flows of mass among four state variables: phosphate (PO_4), phytoplankton (PHYT), zooplankton (ZOOP), and detritus (DET). The mathematical description of the aquatic biogeochemical model is provided in the Appendix A (Table A1), while the definition of the model parameters can be found in Arhonditsis

et al. (2007, 2008b). The phosphate equation considers the phytoplankton uptake, the proportion of the zooplankton excretion and mortality/predation that is returned back to the system as dissolved phosphorus. Epilimnetic phosphate levels are also fuelled by the bacteria-mediated mineralization of detritus, exogenous loading, and are subject to seasonally varying diffusive mixing with the hypolimnion. The equation for phytoplankton biomass considers phytoplankton production and losses due to basal metabolism, settling and herbivorous zooplankton grazing. The growth of phytoplankton is regulated from the physical (light and temperature) conditions and the phosphorus availability. Phytoplankton and detritus are two alternative food sources of zooplankton with equal palatability. Both herbivory and detrivory were formulated using the Holling Type III function, and a sigmoid closure term was selected to represent a "switchable" type of predator behaviour controlled by a prey threshold concentration (Edwards and Yool, 2000). The particulate phosphorus (detritus) is fuelled by phytoplankton respiration, a fraction of the zooplankton growth that represents the faecal pellets, and exogenous loading. Detritus is transformed to phosphate by seasonally forced mineralization processes and sinks out of the epilimnion at a constant rate.

The well-studied system (submodel 1) in the hierarchical model configuration was represented from the average Lake Washington conditions; a mesotrophic system with limnological processes strongly dominated by a recurrent spring diatom bloom with epilimnetic chlorophyll concentration peaks on average at $10\,\mu g\,L^{-1}$, which is approximately three times higher than the summer concentrations when the system is phosphorus limited (Arhonditsis et al., 2003). The hypothetical systems in the second submodel represent oligotrophic conditions, mesotrophic conditions in less intensively studied sites, and eutrophic conditions with monomictic or dimictic mixing patterns, which exchange information via the hierarchical structure with the first submodel. In our analysis, the average input total phosphorus (TP) concentrations for the oligo-, meso-, and eutrophic environments correspond to 50 ($32.5\,\mu g\,TP\,L^{-1}$), 100 ($65\,\mu g\,TP\,L^{-1}$), and 200% ($130\,\mu g\,TP\,L^{-1}$) of the reference conditions in Lake Washington, respectively. Based on these loading scenarios, the model was run using the posterior medians presented in Arhonditsis et al. (2008b). The simulated monthly averages provided the mean values of normal distributions with standard deviations assigned to be 15% of the monthly values for each state variable (Zhang and Arhonditsis, 2008). These distributions were then sampled to generate the oligo-, meso- and eutrophic datasets used for the Bayesian model calibration along with the corresponding hypolimnetic phosphate boundary conditions.

2.3. Numerical approximations for posterior distributions

The calibration vector consists of the same 14 parameters used in previous applications of the model (Arhonditsis et al., 2007, 2008b). The prior distributions of the hyperparameters or global priors were formulated on the basis of existing knowledge (e.g., field observations, laboratory studies, literature information and expert judgment) of the relative plausibility of their values. In this study, we identified the global minimum and maximum values for each parameter, and then we assigned lognormal distributions parameterized such that 95% of the parameter values were lying within the literature ranges (Steinberg et al., 1997). The global prior distributions of the model parameters are presented in Table 2. The numerical approximations of the posterior distributions were obtained using the general normal-proposal Metropolis algorithm along with an ordered overrelaxation (Spiegelhalter et al., 2003). This MCMC scheme generates multiple samples per iteration and reduces the within-chain correlations by selecting a value that is negatively correlated with the current one of each stochastic node (Neal, 1998). The posterior simulations were based on one chain with starting point a vector obtained from an earlier optimization of the model with the Fletcher–Reeves conjugate-gradient method (Chapra and Canale, 1998). We used 50,000 iterations and convergence was assessed with the modified Gelman–Rubin convergence statistic (Brooks and Gelman, 1998). Our framework was implemented in the WinBUGS Differential Interface (WBDiff); an interface that allows numerical solution of systems of ordinary differential equations (ODEs) within the WinBUGS software. The ODEs were solved using the fourth-order Runge-Kutta method.

2.4. Model updating

We used the MCMC estimates of the mean and standard deviation parameter values along with the covariance structure to update the model (Legendre and Legendre, 1998). Under the assumption of a multinormal distribution for the log-transformed parameter values, the conditional distributions are given by:

$$\hat{\theta}_{i|j} = \hat{\theta}_i + [\theta_j - \hat{\theta}_j]\Sigma_j^{-1}\Sigma_{i,j} \tag{15}$$

$$\Sigma_{i|j} = \Sigma_i - \Sigma_{j,i}\Sigma_j^{-1}\Sigma_{i,j} \quad j \in \{i+1, \ldots, n\} \tag{16}$$

where $\hat{\theta}_{i|j}$ and $\Sigma_{i|j}$ correspond to the mean value and the dispersion matrix of the parameter i conditional on the parameter vector j; the values of the elements Σ_i $\Sigma_{i,j}$ and Σ_j correspond to the variance and covariance of the two subset of parameters; and $\hat{\theta}_i, \hat{\theta}_j, \theta_j$ correspond to the posterior mean and random values of the parameters i and j, respectively. The shape and scale parameters of the inverse-gamma distributions used to represent our updated beliefs for the values of the seasonally invariant discrepancy terms (Eq. (11)) were estimated with the method of moments (Bernardo and Smith, 1994 p. 434). We also examined the sensitivity of our results to these informative priors using alternative ones that reflected lower confidence in the estimated error term values (Qian and Reckhow, 2007).

3. Results

3.1. General patterns of the posterior parameter distributions

The MCMC sequences of the models converged rapidly (≈5000 iterations) and the statistics reported herein were based on the last 45,000 draws by keeping every 10th iteration (thin = 10). The evaluation of the degree of updating of model input parameters was based on the shifts of the most possible values and the reduction of the parameter uncertainty. The relative differences between global priors and scenario/submodel-specific posterior estimates of the mean values and standard deviations of the 14 model parameters are presented in Fig. 2. The majority of the parameters were characterized by significant shifts of their posterior means relative to the global priors assigned to the first four scenarios (*A, B, C*, and *D*). Some parameters showed an increase of their central tendency values in all the scenarios examined, e.g., the phytoplankton respiration rate (r) (15–81%), the zooplankton mortality rate (d) (5–165%), and the zooplankton grazing half-saturation constant (μ) (16–182%). There were also parameters with consistently decreased posterior mean values, such as the detritus sinking rate (ψ) (54–84%), the detritus mineralization rate (φ) (17–79%), and the zooplankton excretion fraction (β) with 14–39% decrease. Notably, the mean values of some parameters significantly varied among the different scenarios, e.g., the phytoplankton sinking loss rate (s) (−68 to 172%), the half-saturation constant for predation (pred) (−18–149%), and the regeneration of zooplankton predation excretion (γ) with −26%

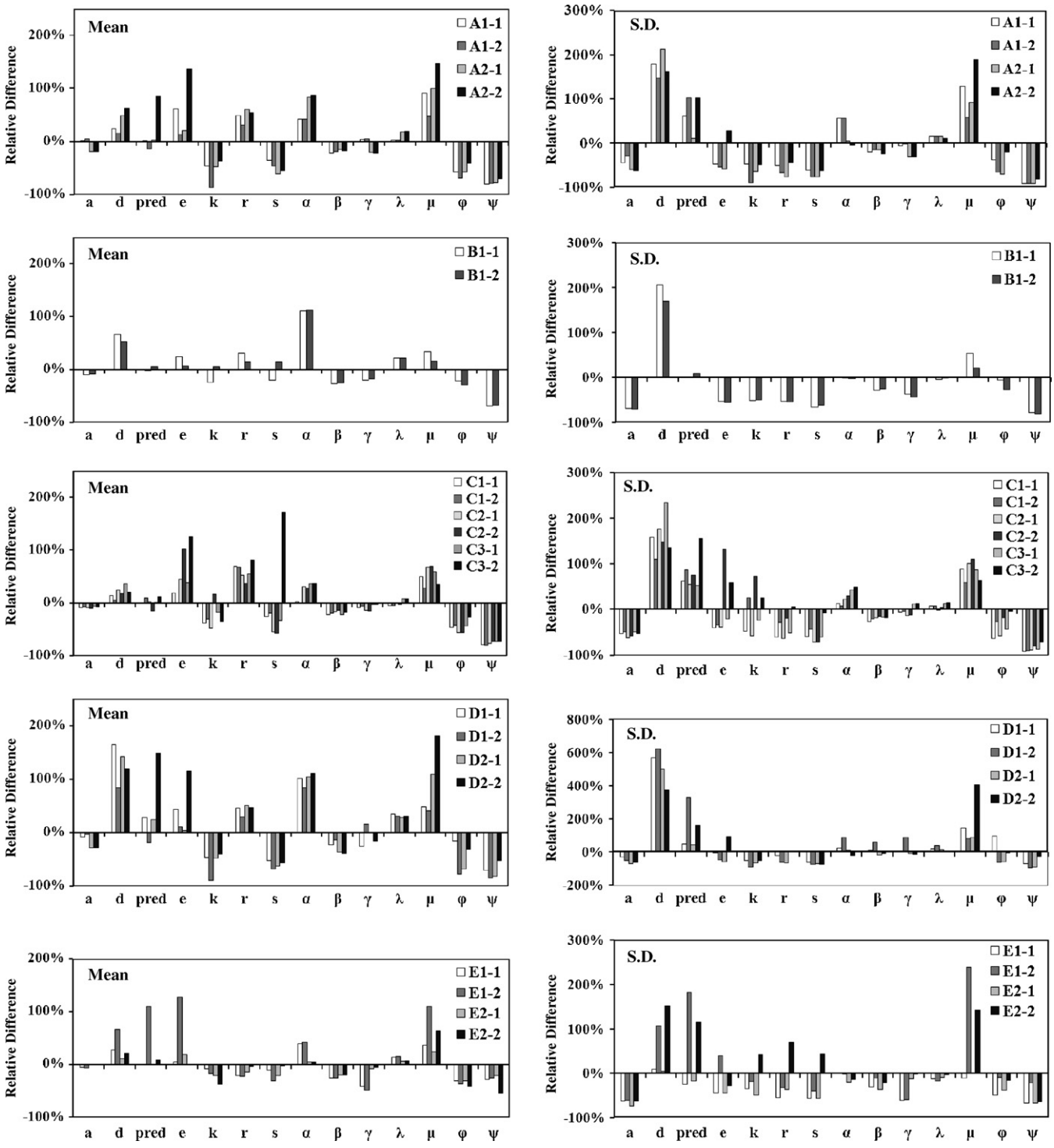

Fig. 2. The relative difference between posterior estimates of the mean values and standard deviations and the corresponding global prior distributions of the model parameters. Relative difference$_{ij}$ = (Posterior$_{ij}$ − Prior)/Prior × 100%, i = scenario and j = submodel (see the first two columns in Table 1).

to 15% relative change. The majority of the posterior standard deviations decreased relative to the values assigned to the hyper-parameters, such as the maximum phytoplankton growth rate (a) (30–72%), the phytoplankton sinking loss rate (s) (8–78%), and the detritus sinking rate (ψ) (27–93%). However, there were also cases with significantly increased posterior standard deviations and the most characteristic examples were the zooplankton mortality rate (d) (110–620%), the half-saturation constant for predation (pred) (1–329%), and the zooplankton grazing half-saturation constant (μ) (20–404%).

3.2. What is the effect of the hierarchical configuration on the posterior parameter distributions?

We also compare the posterior parameter patterns when the model was calibrated against individual datasets representing oligo-, meso-, and eutrophic conditions (see Appendix A: Table A2) and those obtained when crossing sites of different trophic states under the hierarchical framework, i.e., scenarios *A* and *D* (Fig. 3). [The MCMC estimates of the mean values and standard deviations of the model stochastic nodes (parameters and error terms) derived

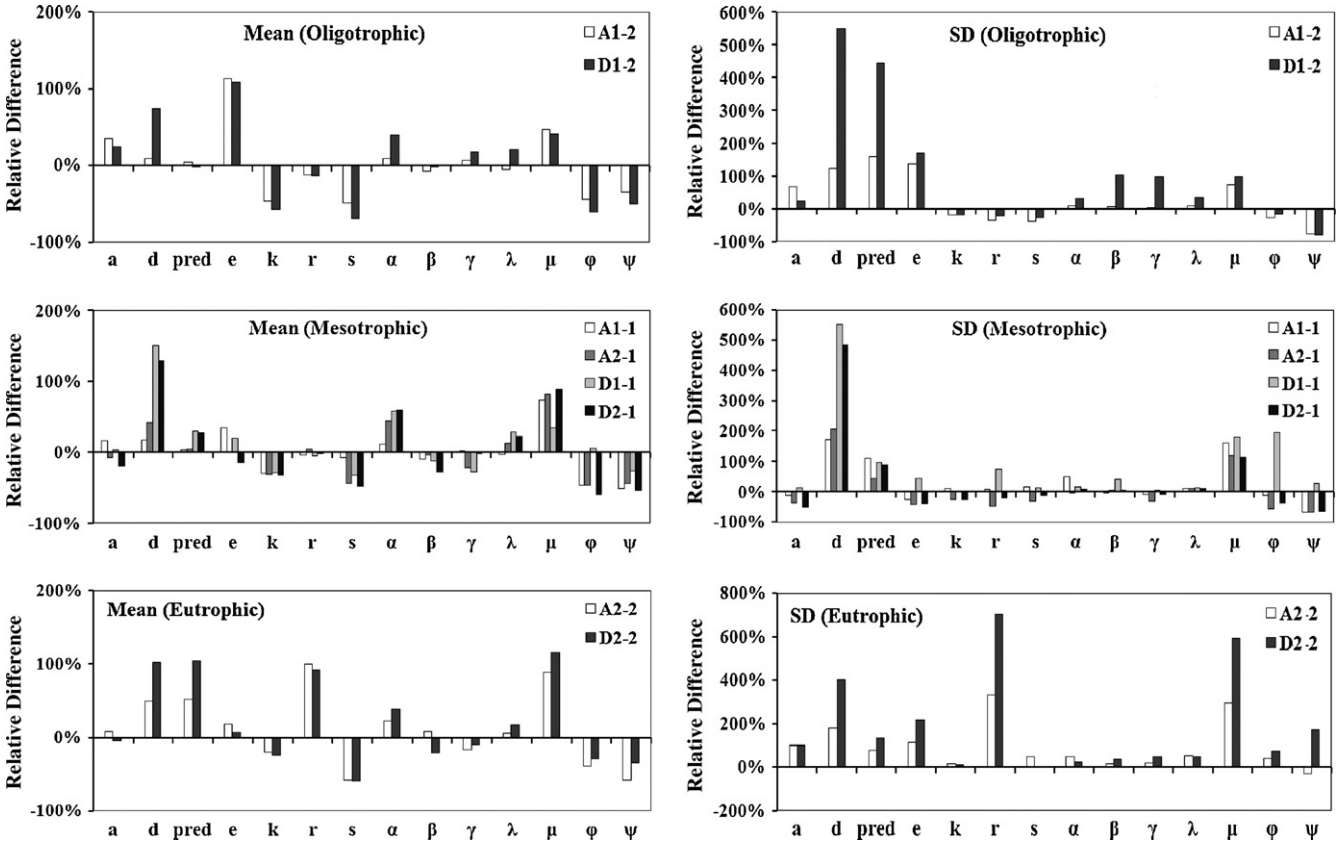

Fig. 3. The relative difference between the posterior parameter estimates obtained after model calibration against individual datasets representing oligo-, meso- and eutrophic conditions and the hierarchical settings examined in the scenarios *A* and *D*. Relative difference$_i$ = (Hierarchical$_i$ − Nonhierachical$_i$)/Nonhierachical$_i$ × 100%, *i* = oligotrophic, mesotrophic, eutrophic.

from the first and fourth scenarios are provided in Tables A3 and A5.] An important finding was that the previously reported inflation of the standard deviation of parameters associated with the zooplankton feeding kinetics (μ) and mortality (d, pred) is only manifested with the hierarchical setting. We also note the significant increase of the posterior means of the same parameters in the mesotrophic and –especially– the eutrophic submodels. Generally, the relaxation of the prior precisions of the system-specific parameters and the broadening of the sampled parameter space (scenario *D*) resulted in higher posterior standard deviations. The phytoplankton respiration rate (r) demonstrated significant increase of the first and second order moments relative to the estimates obtained when the model was calibrated against the eutrophic dataset. The same trend was observed with the half-saturation constant for PO_4 uptake (e) in the two oligotrophic submodels. The latter cases were also characterized by a consistent decrease of the central tendency and dispersion values of the cross-thermocline exchange rate (k), the phytoplankton respiration (r) and sinking

Table 3
Scenario C. Markov Chain Monte Carlo posterior estimates of the mean values and standard deviations of the model stochastic nodes.

Nodes	C_1				C_2				C_3			
	1		2		1		2		1		2	
	Mean	S. D.	Mean	S. D.	Mean	S. D.	Mean	S. D.	Mean	S. D.	Mean	S. D.
a	1.314	0.140	1.330	0.158	1.307	0.116	1.306	0.128	1.361	0.157	1.331	0.140
d	0.197	0.055	0.182	0.045	0.216	0.059	0.203	0.053	0.234	0.072	0.209	0.050
pred	54.37	22.64	59.25	26.09	56.24	21.58	46.43	24.41	55.26	21.21	60.84	35.64
e	13.05	2.895	10.92	3.122	15.84	2.907	22.11	11.17	15.09	3.815	24.64	7.687
k	0.022	0.007	0.025	0.016	0.019	0.005	0.043	0.022	0.030	0.010	0.024	0.016
r	0.197	0.027	0.197	0.050	0.178	0.025	0.161	0.057	0.181	0.034	0.211	0.075
s	0.030	0.013	0.033	0.018	0.018	0.009	0.017	0.009	0.027	0.013	0.110	0.029
α	0.376	0.143	0.360	0.136	0.481	0.154	0.471	0.162	0.497	0.180	0.502	0.187
β	0.229	0.081	0.237	0.088	0.245	0.091	0.252	0.095	0.230	0.092	0.240	0.092
γ	0.266	0.104	0.275	0.105	0.253	0.096	0.248	0.097	0.286	0.123	0.284	0.126
λ	0.581	0.115	0.576	0.114	0.599	0.107	0.593	0.112	0.659	0.121	0.660	0.124
μ	9.896	3.529	8.453	2.968	11.01	3.752	11.15	3.929	10.47	3.496	8.886	3.044
φ	0.050	0.011	0.053	0.023	0.040	0.013	0.040	0.026	0.052	0.018	0.067	0.030
ψ	0.030	0.006	0.028	0.008	0.033	0.008	0.038	0.016	0.038	0.010	0.038	0.023
σ_{PO_4}	0.796	0.335	1.383	1.230	0.712	0.303	1.024	0.638	0.709	0.316	5.666	6.063
σ_{PHYT}	8.516	12.13	7.062	15.21	6.906	9.113	9.520	18.30	8.727	11.70	246.7	153.3
σ_{ZOOP}	28.79	12.69	7.989	13.97	24.63	12.19	33.45	23.59	22.80	12.78	68.76	63.26
σ_{DET}	2.261	1.072	1.486	1.926	2.568	1.234	2.904	2.384	2.637	1.471	15.71	7.939

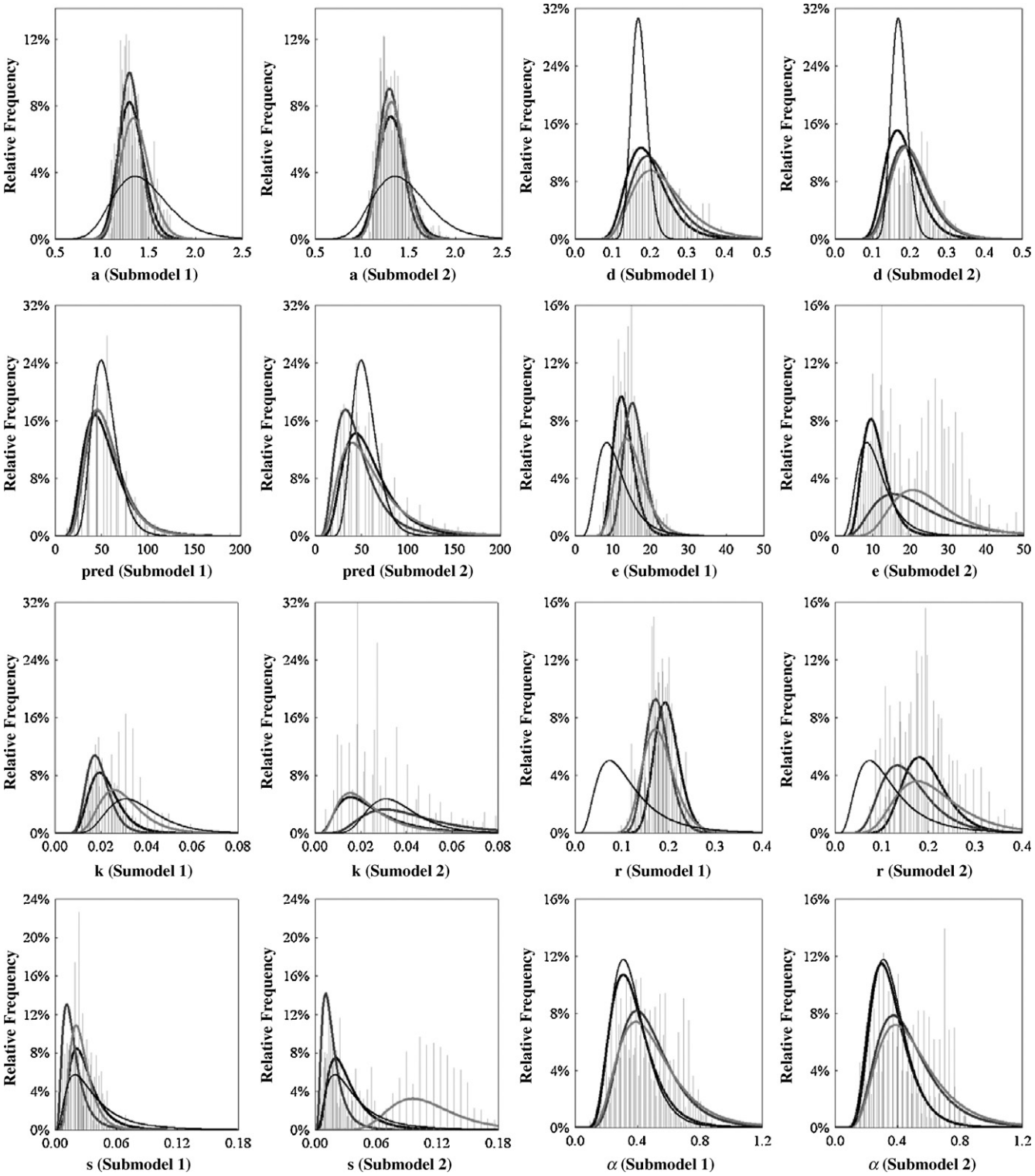

Fig. 4. *Scenario C.* Prior (thin black lines) and posterior (C_1: thick black lines; C_2: thick grey lines; and C_3: thick light grey lines) parameter distributions.

loss rates (s), the detritus remineralization (φ) and sinking rates (ψ).

3.3. Examination of the posterior patterns when combining systems and/or sites with different sampling intensity (C_1 and C_2) or systems with different hydrodynamics (C_3)

The posterior estimates of the mean values and standard deviations of the 14 model parameters with the third scenario are shown in Table 3 and Fig. 4. The first sub-scenario (C_1) aimed to combine two datasets representing similar dynamics but different sampling intensity, i.e., 12 monthly values versus four seasonal averages for each state variable. Our results show that the posterior means and standard deviations of the two submodels were very similar. Relatively similar results were also found with the second sub-scenario (C_2), i.e., data collected on a monthly basis during the stratified period, although some variation exists with regards to the posterior moments of the cross-thermocline exchange rate

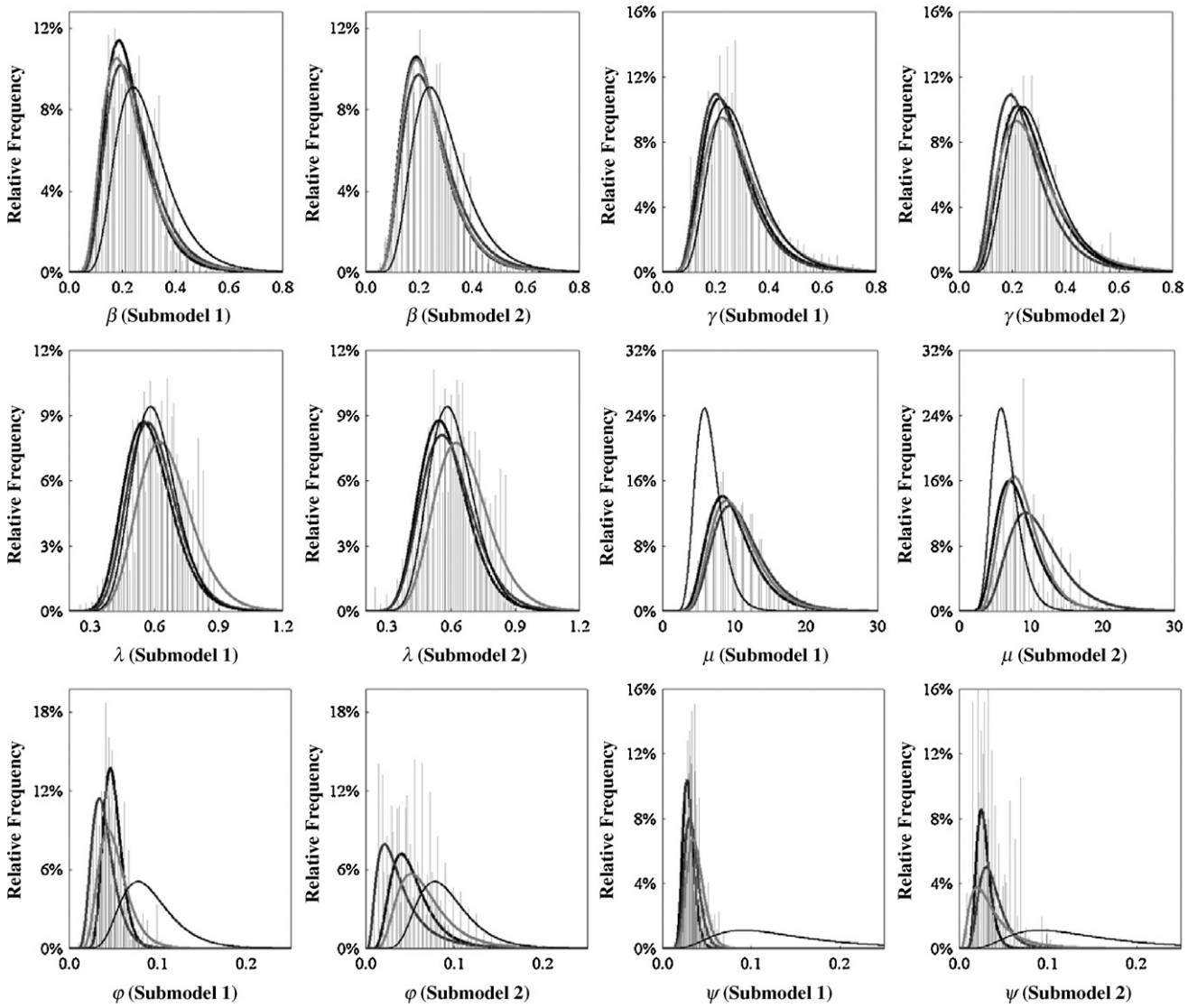

Fig. 4. (*Continued*).

(k), the half-saturation constant for PO_4 uptake (e), and the phytoplankton respiration rate (r). The same parameters along with the half-saturation constant for predation (pred), the zooplankton grazing half-saturation constant (μ), and the phytoplankton sinking velocity (s) were moderately (or significantly) different when examining systems with different trophic states and vertical mixing regimes, i.e., mesotrophic monomictic versus eutrophic dimictic lakes. The temporally invariant error terms ($\sigma_j, j = PO_4$, PHYT, ZOOP, DET) delineate a constant zone around the model predictions that accounts for the discrepancy between model structure and natural system dynamics. The first and second order moments of the posterior distributions of the error terms associated with the model predictions in the "well-studied" system were fairly constant across the three scenarios (C_{11}, C_{21}, and C_{31}). Interestingly, lower error values were found when the model was calibrated against seasonal data (C_{12}), whereas the use of data collected only from the stratified period increased the model error (scenario C_{22}); especially for the zooplankton biomass (σ_{ZOOP} with mean and standard deviation equal to 33.45 and 23.59 $\mu g\,C\,L^{-1}$, respectively). The scenario C_{32} of the eutrophic dimictic lake resulted in very high error values; in particular, the error terms associated with phytoplankton (σ_{PHYT} with a mean of 246.7 $\mu g\,C\,L^{-1}$ and a standard deviation of 153.3 $\mu g\,C\,L^{-1}$) and zooplankton biomass (σ_{ZOOP} with mean and standard deviation equal to 68.76 and 63.26 $\mu g\,C\,L^{-1}$, respectively).

Generally, the comparison between the observed and posterior predictive monthly distributions indicates that the plankton models calibrated under the Bayesian hierarchical structure provided accurate system representations for all the scenarios examined. In particular, the mesotrophic submodel of the third scenario resulted in median predictions along with 95% credible intervals that closely describe the observed data, despite the slight underestimation of the spring plankton biomass peaks (Fig. 5). We also highlight the robustness of the model predictions of the same submodel, regardless of the second dataset considered under the hierarchical framework. On the other hand, the median model predictions for chlorophyll *a*, zooplankton, phosphate and total phosphorus matched the seasonal data (scenario C_{12}), except from the zooplankton mean spring biomass. In the same scenario, the wider uncertainty bands reflect the higher variability (measurement error) associated with the seasonal average values. The calibration of the second submodel against the dataset from the stratified period resulted in close reproduction of the summer plankton biomass levels as well as the contemporaneous phosphorus variability (scenario C_{22}). Finally, the median predictions along with the uncertainty bounds delineated a zone that closely represented the

dynamics of the eutrophic dimictic system during the open surface period (scenario C_{32}).

3.4. Examination of the posterior patterns when combining a "refined" parameterization (updated model) stemming from a well-studied system with a less intensively studied system

The parameter posterior statistics along with the model error terms with global priors based on the updated conditional distributions of the 14 parameters along with informative inverse-gamma distributions for the seasonally invariant discrepancy terms are presented in Table 4 and Fig. 6. The posterior means and standard deviations of the updated model remained fairly stable under the two sub-scenarios E_1 and E_2 examined. It should also be noted that the shifts of the posterior means were less than 40% relative to the updated global priors, whereas the majority of the standard deviations were significantly reduced (see also Fig. 2). On the other hand, the calibration of the second model with an eutrophic dataset (scenario E_{12}) resulted in posteriors alike those obtained for the first submodel. Notable exceptions were the half-saturation constant for PO_4 uptake (e), the zooplankton grazing half-saturation constant (μ), and the half-saturation constant for predation (pred). Furthermore, in a similar manner to the scenario C_1, the use of four seasonal averages provided very similar posterior means and standard deviations between the two submodels (Scenario E_{22}). The same scenario also resulted in fairly low mean values of the model error terms, although the corresponding coefficients of variation (standard deviation/mean) were much higher. The same high coefficients of variation characterized the model error terms (σ_j) of the scenario E_{12}, but the posterior means were

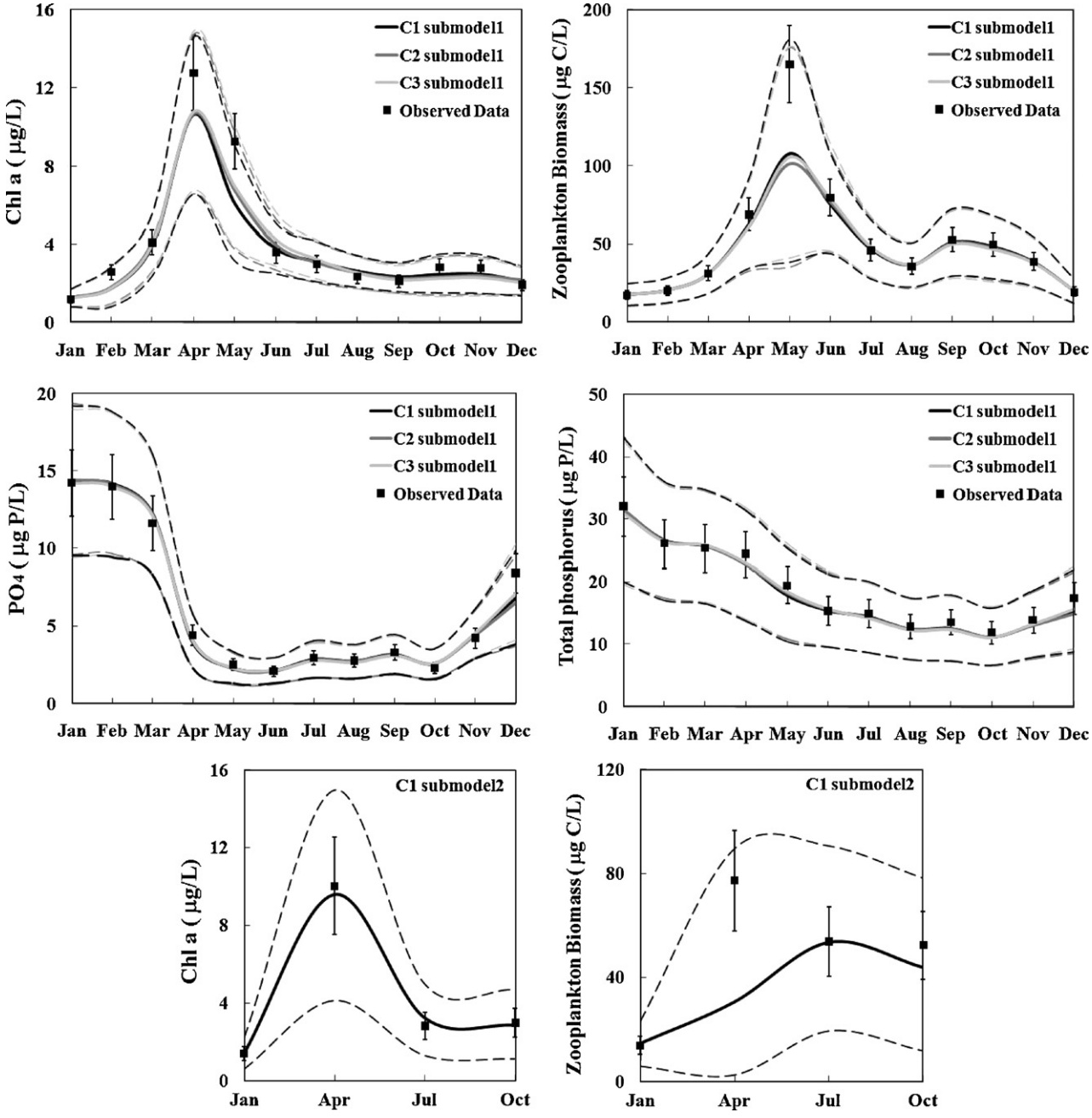

Fig. 5. *Scenario C.* Comparison between the observed and posterior predictive distributions. Solid line corresponds to the median value of model predictions and dashed lines correspond to the 2.5% and 97.5% uncertainty bounds. The square dots represent the observed data, while the error bars reflect the measurement error.

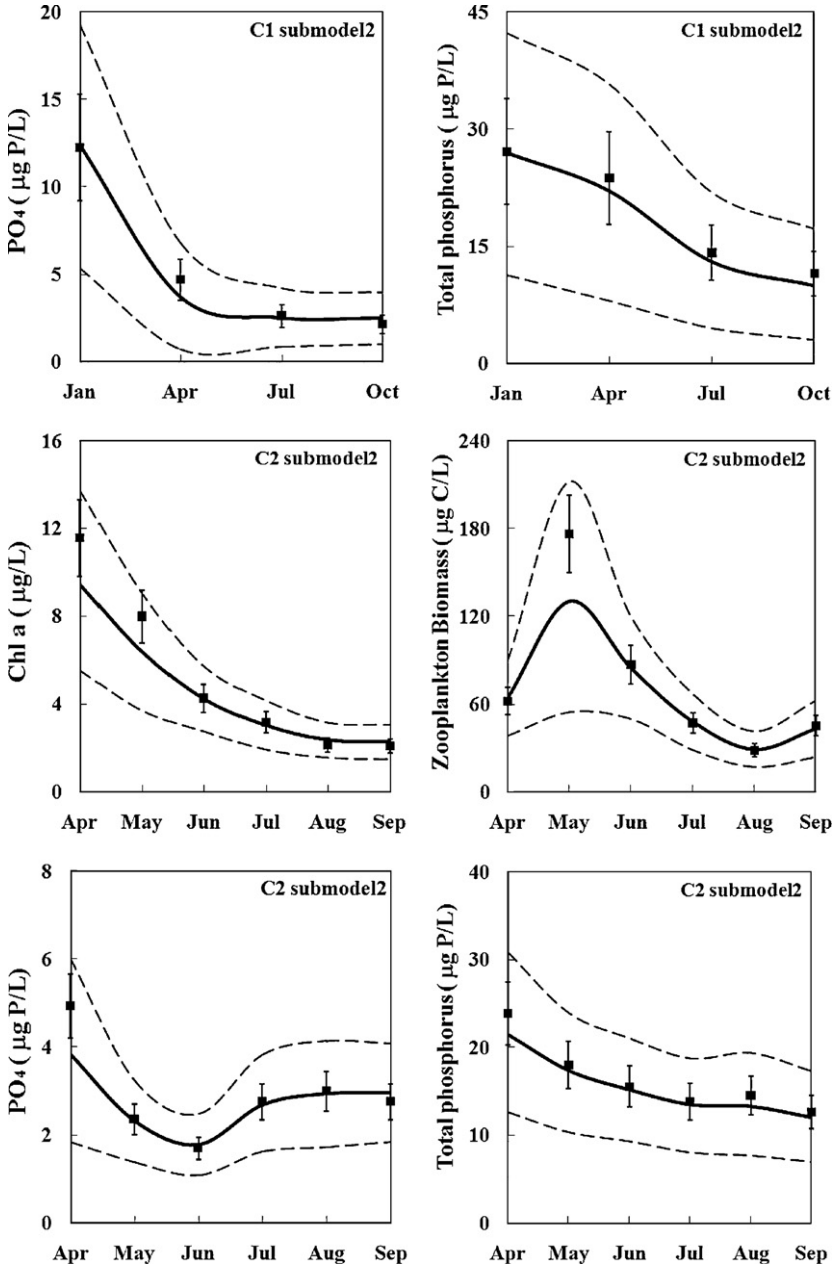

Fig. 5. (*Continued*)

also significantly higher than the ones obtained for the updated model (E_{11}).

In the fifth scenario, the predictive median values along with the uncertainty bounds of the updated model provided results similar to those obtained from the submodel 1 of the third scenario and all the observed monthly values were included within the 95% credible intervals (Fig. 7). However, the zooplankton median predictions still underestimated the late spring biomass, which was also the case with the second submodel of the scenario E_1, i.e., eutrophic dataset with 12 monthly observations. The latter scenario resulted in a notably accurate reproduction of the chlorophyll *a*, total phosphorus, and phosphate seasonal cycle. Finally, the use of updated global priors did not improve model fit against the dataset that consists of four seasonal averages (E_{22}). The wide prediction bounds included all the observed values, but the median spring zooplankton predictions failed again to capture the concurrent observed biomass levels.

4. Discussion

The philosophical and pragmatic differences between Bayesian and frequentist methods of inference have been extensively debated in the ecological literature (Dennis, 1996; Ellison, 1996, 2004). The distinctions arise from the different definitions of probability (long-run relative frequencies of events vis-á-vis an individual's degree of belief in the likelihood of an event), the use of prior knowledge along with the sample data, and the treatment of model parameters as random variables or as fixed quantities (Ellison, 2004). Recently, however, Clark (2003, 2005) offered a different perspective arguing that the assumptions of frequentist and simple Bayesian models are more similar than are usually perceived in ecological studies and that only the hierarchical Bayes is a distinctly different framework to accommodate the complexity in environmental systems. Hierarchical Bayes relaxes the fundamental assumption that there is an underlying "true"

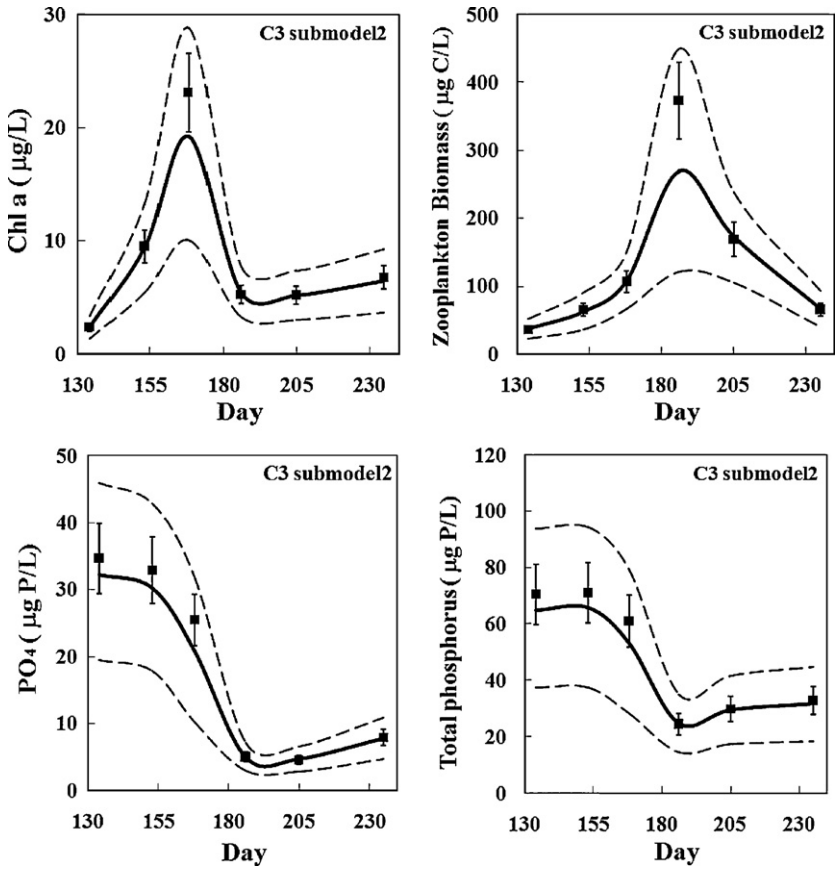

Fig. 5. (*Continued*).

parameter value that is gradually approximated with increasing sample size. Using simple empirical models with a large number of hierarchies and spatiotemporally variant parameters, the latter feature has been shown to provide an effective means for addressing difficult space-time problems (Borsuk et al., 2001; Wikle, 2003a; Malve and Qian, 2006). Our objective herein was to demonstrate how the hierarchical Bayes can be used to simultaneously calibrate mathematical models at multiple sites with different ecological dynamics or amount of information available.

Table 4
Scenario E. Markov Chain Monte Carlo posterior estimates of the mean values and standard deviations of the model stochastic nodes.

Nodes	E_1				E_2			
	1		2		1		2	
	Mean	S. D.	Mean	S. D.	Mean	S. D.	Mean	S. D.
a	1.209	0.069	1.195	0.071	1.271	0.048	1.271	0.068
d	0.234	0.024	0.303	0.045	0.204	0.023	0.222	0.055
pred	54.23	7.908	113.0	29.71	53.49	8.616	58.62	22.62
e	13.87	1.856	30.08	4.635	15.62	1.811	13.02	2.377
k	0.026	0.004	0.023	0.005	0.022	0.003	0.018	0.008
r	0.143	0.014	0.150	0.021	0.154	0.019	0.174	0.053
s	0.025	0.005	0.020	0.006	0.022	0.005	0.027	0.016
α	0.655	0.131	0.665	0.129	0.496	0.104	0.494	0.114
β	0.192	0.061	0.191	0.078	0.207	0.055	0.208	0.069
γ	0.174	0.043	0.152	0.045	0.273	0.098	0.283	0.111
λ	0.730	0.097	0.743	0.091	0.685	0.100	0.686	0.105
μ	9.984	1.429	15.34	5.493	9.026	1.628	11.910	3.935
φ	0.050	0.011	0.046	0.019	0.051	0.013	0.043	0.018
ψ	0.040	0.006	0.041	0.016	0.044	0.007	0.026	0.007
σ_{PO_4}	0.893	0.290	1.658	0.778	0.800	0.258	1.000	0.959
σ_{PHYT}	2.962	4.822	10.24	16.32	3.113	5.194	7.964	17.29
σ_{ZOOP}	14.50	4.151	21.37	10.56	16.75	5.412	8.158	14.34
σ_{DET}	4.312	1.037	9.673	3.210	4.136	0.959	1.461	1.947

4.1. How robust are the posterior patterns under the hierarchical framework?

The degree of updating of the model input parameters from prior to posterior is usually evaluated using three different criteria: (i) shift in the most likely value; (ii) reduction in the parameter uncertainty; and (iii) change in the shape of the distribution (Endres and Schindelin, 2003). In this study, although we have not quantified the change in the shape from prior to posterior parameter distributions, the first two criteria did reveal interesting results with regards to the degree of updating under the hierarchical model configuration. First, we highlight the often significant shifts of the posterior means and the increased standard deviations of the zooplankton mortality rate (d), the half-saturation constant for predation (pred), and the zooplankton grazing half-saturation constant (μ). These posterior patterns probably indicate that the zooplankton feeding kinetics and the mortality/higher predation rates (the so-called closure term) are primarily used to accommodate the site-specific variability, and therefore can be more resistant to the Bayesian shrinkage effect. Shrinkage is a well-known phenomenon in both Bayesian and frequentist statistics in which individual estimates are shrunk toward the overall mean when they are derived jointly rather than independently (Efron and Morris, 1975; Gelman and Pardoe, 2006). This finding reiterates the well-documented profound impact of these parameters upon the dynamics of plankton ecosystem models and underscores the importance of developing articulate site-specific prior probability distributions when data from different study sites are combined under the hierarchical

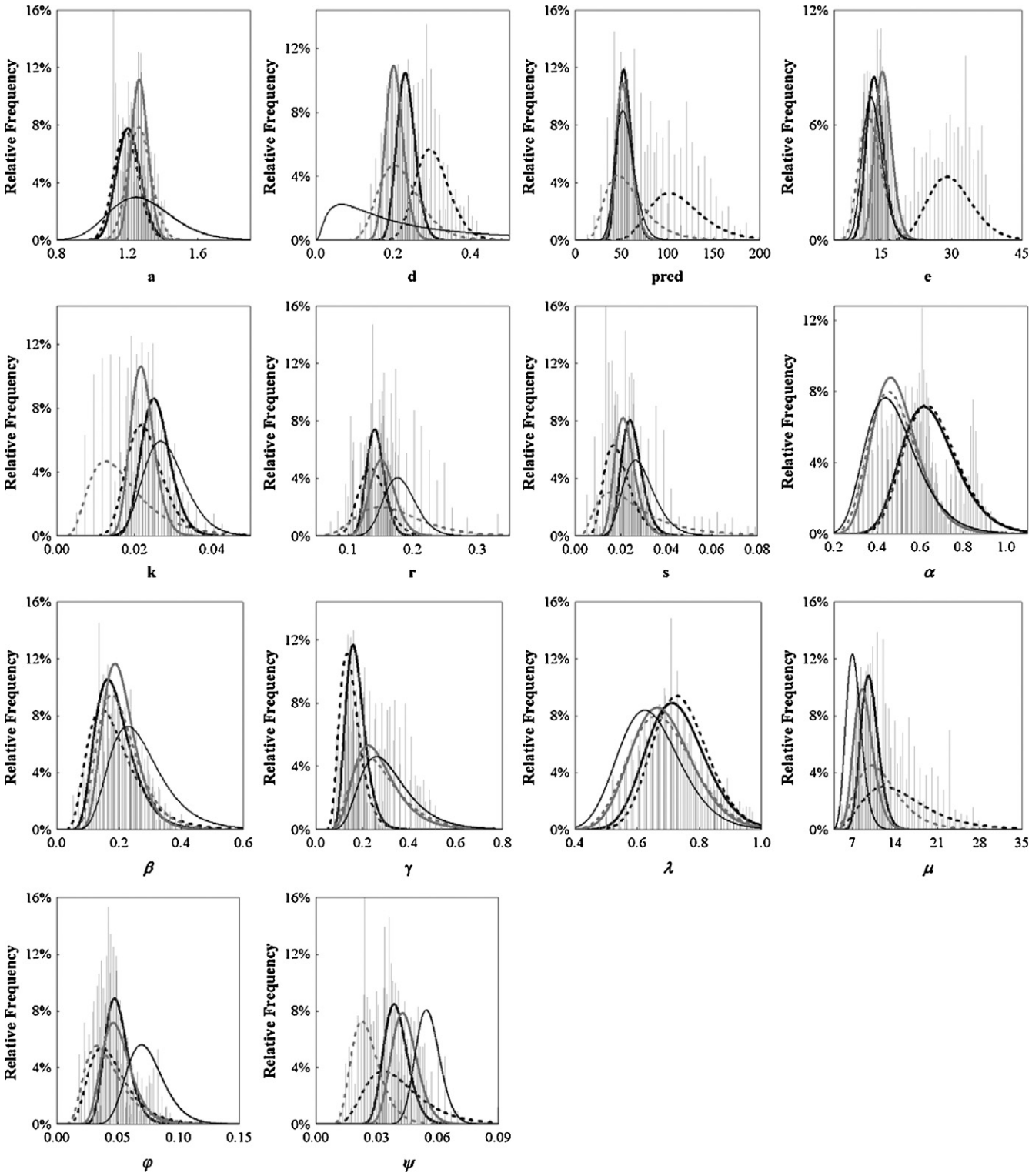

Fig. 6. *Scenario E.* Prior (thin black lines) and posterior (E_1 submodel 1: thick black lines; E_1 submodel 2: thick black dashed lines; E_2 submodel 1: thick gray lines; and E_2 submodel 2: thick dashed grey lines) parameter distributions.

structure (Edwards and Yool, 2000; Franks, 2002; Arhonditsis and Brett, 2004).

The rest parameters of the calibration vector can be classified into two groups: (i) parameters that depending on the scenario examined can play an active role during the model training process, e.g., the half-saturation constant for PO_4 uptake (e), phytoplankton respiration (r) and sinking (s) rates, the detritus sinking (ψ) and mineralization (φ) rates; (ii) parameters with relatively unaltered posterior moments comparing with the values assigned to the global priors, e.g., the zooplankton growth efficiency (a) and excretion fraction (β), and the regeneration of zooplankton predation excretion (γ). Overall, these results are similar to those reported in earlier applications of the same simple model structure (Arhonditsis et al., 2007, 2008b). The consistent increase/decrease of the central tendency values of some parameters, such as the phytoplankton respiration rate (r), the detritus sinking rate (ψ), and the

detritus mineralization rate (φ), probably indicates that the prior distributions obtained from the literature review misrepresented the underlying ecological processes; at least under the setting (e.g., datasets, model structure) used in this analysis. We also note the relatively greater shifts in the mean parameter values when relaxing our confidence in the prior knowledge used to formulate the global priors (scenario *D*). The sensitivity of the first-order posterior moments to the assigned site-specific parameter precisions suggests that the broadening of the parameter space examined allows the identification of regions of higher model performance but also increases the standard deviations of the parameter marginal distributions (see the differences of the parameter standard deviations between the scenarios *A* and *D* in Figs. 2 and 3).

4.2. How can the hierarchical framework assist the current modeling practices?

The Bayesian hierarchical proposition may be useful for a variety of aquatic science and ecological modeling applications in which partial, but not complete, commonality can be assumed among the modeled units. A characteristic case is the Laurentian Great Lakes region where the most degraded areas are nearshore zones above the summer thermocline adjacent to the mouths of large rivers and enclosed bays/harbours with restricted mixing with offshore water. These areas are intermediate zones in that they receive highly polluted inland waters from watersheds with significant agricultural, urban, and/or industrial activities while mixing

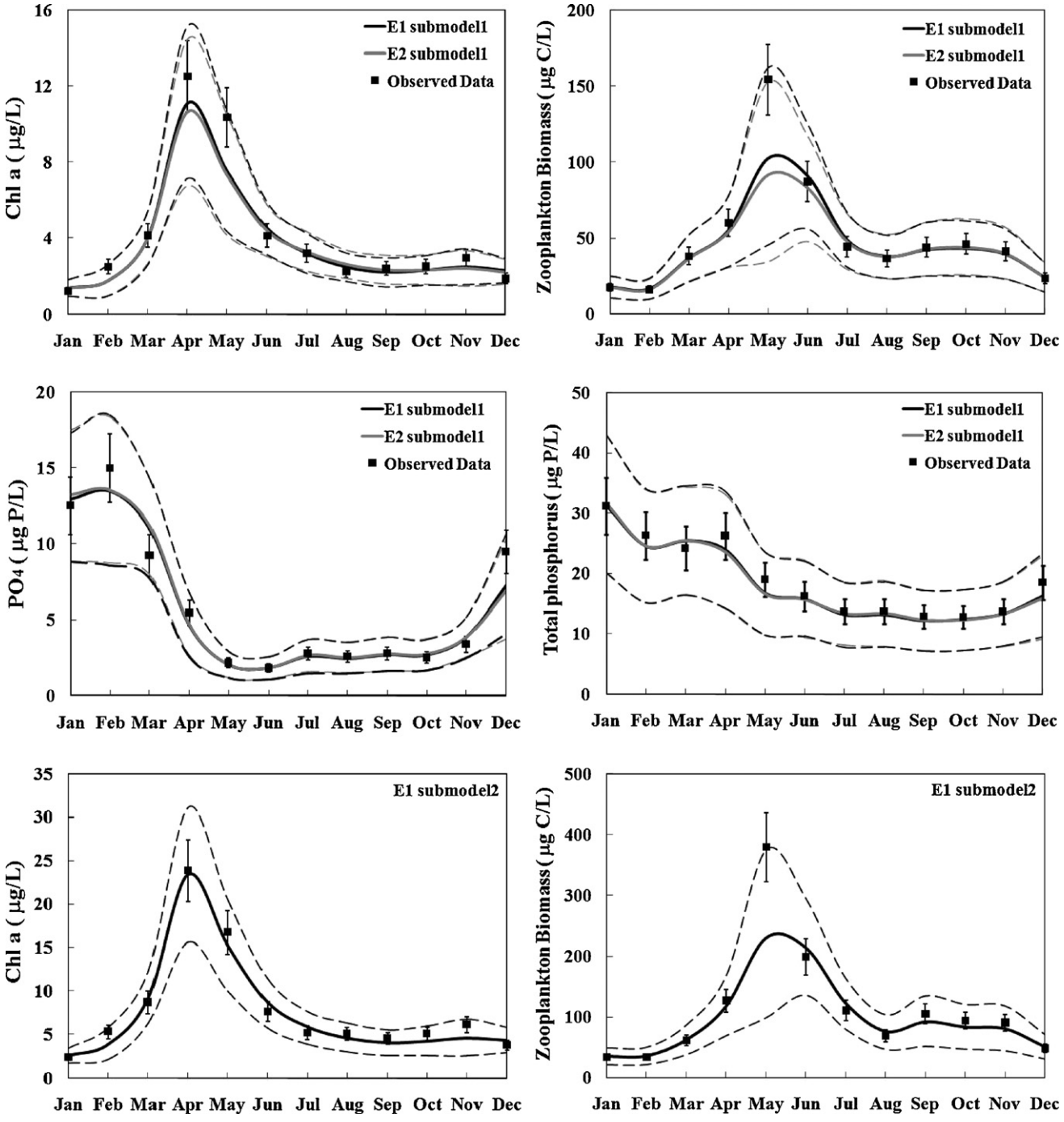

Fig. 7. *Scenario E.* Comparison between the observed and posterior predictive distributions. Solid line corresponds to the median value of model predictions and dashed lines correspond to the 2.5% and 97.5% uncertainty bounds. The square dots represent the observed data, while the error bars reflect the measurement error.

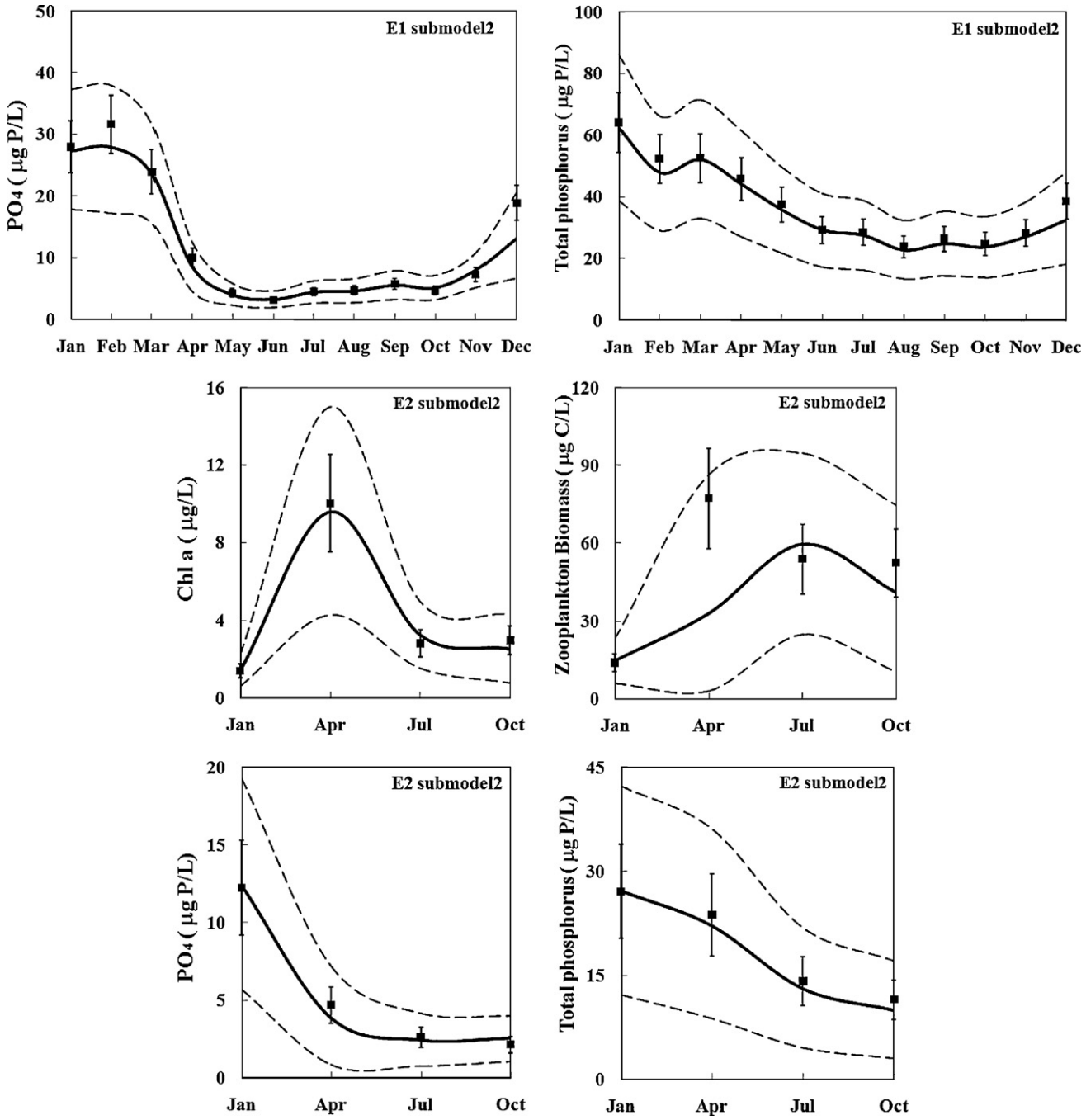

Fig. 7. (*Continued*).

with offshore waters having different biological and chemical characteristics (Nicholls, 1999; Rockwell et al., 2005; Winter et al., 2007). We believe that this type of spatial heterogeneity cannot be fully accommodated by the typical practice of developing spatially explicit mechanistic models with common parameter values over the entire systems; that is, how realistic is to assume that the same phytoplankton growth rate occurs throughout the waterbody? Rather, the practical compromise between entirely site-specific and globally common parameter estimates offered by the hierarchical approach may be a conceptually more sound strategy (Fig. 8). Importantly, our illustration showed that such model configuration does not negate the basic premise for using process-based models, i.e., reproduction of the observed system dynamics while gaining mechanistic insights, and it does provide parameter posteriors that have meaningful ecological interpretation. For example, the posterior means for the half-saturation constant for PO_4 uptake (e) after updating the model against individual datasets representing oligo-, meso-, and eutrophic conditions were equal to 5.75, 13.17, and 22.05 $\mu g\,P\,L^{-1}$, respectively (Table A2). These values are ecologically plausible and depict the continuum between phytoplankton communities dominated by species with strong (e.g., diatom-like) and weak (e.g., cyanobacteria-like) P competitive abilities. With the hierarchical scheme, the relative magnitude of the same parameter remained unaltered across the three states, although their absolute values were somewhat different (Tables A3 and A5). The wider observational range stemming from the combination of sites that represent different trophic conditions (scenarios *A* and *D*) consistently reduced the error terms associated with the phosphate (σ_{PO_4})

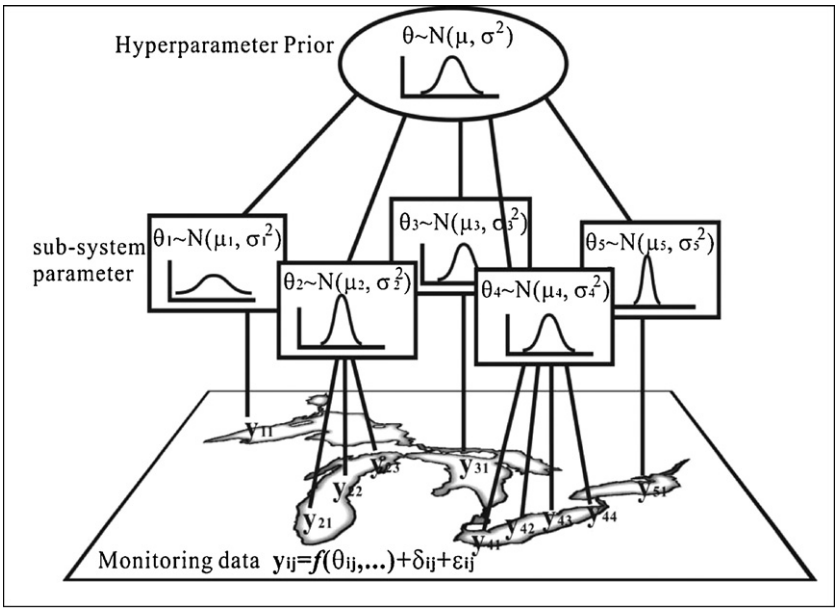

Fig. 8. A conceptual application of the Bayesian hierarchical framework to allow the transfer of information in space.

and detritus (σ_{DET}) equations, whereas variant results were found for the phytoplankton (σ_{PHYT}) and zooplankton (σ_{ZOOP}) error terms depending on the scenarios examined. Realistic parameter values and reduced error terms were also derived from the second experiment that simulated the case in which inshore and offshore areas of a mesotrophic lake are combined under the hierarchical structure (Table A4).

We also examined the ability of the Bayesian hierarchical framework to provide a mechanism for pooling information from systems with different sampling intensity and strengthen the predictive ability in individual sites. Indeed, our analysis showed that primarily the scenario that uses seasonal averages for the state variables (C_1) and secondarily the one using data solely from the stratified period (C_2) resulted in relatively similar posterior parameter moments between the two locations, providing more confidence in the representation of the ecological structure of the less intensively studied site. Furthermore, aside from the previously mentioned low precisions of the parameters associated with the zooplankton feeding kinetics and mortality rates, the differences between the posterior first and second order moments of the hyperparameters and the system-specific parameters were also quite small (Fig. 9); that is, the site-specific parameters converged toward the global means but these shifts were not accompanied by a significant shrinkage of the corresponding parameter standard deviations (Gelman and Pardoe, 2006).

The comparison between the observed and posterior predictive monthly distributions along with the values of the error terms can also be used to dictate the optimal type of information required to improve the predictive power of the model. For example, the calibration of the model with data collected once per season results in very wide uncertainty bands and thus less useful for water quality management. Furthermore, although the median predictions closely match the majority of the observed data and the values of the error terms were notably lower, the model fails to capture the timing of the spring phytoplankton bloom and does not reproduce the contemporaneous peak of the zooplankton biomass. Interestingly, the latter problems were not alleviated when the model of the less intensively studied system was combined with a "refined" model parameterization based on a well-studied site (scenario *E*). On the other hand, the use of data collected with higher frequency but solely from the stratified period overcomes the misrepresentation of the spring plankton dynamics and also reduces the predictive uncertainty. Similar experiments can be designed regarding the spatiotemporal sampling intensity or the collection of data on parameters versus data on output variables, while the subsequent assessment of the value of information can further optimize the existing monitoring programs and assist model-based decision making and management (Dorazio and Johnson, 2003). Finally, we note the overwhelmingly high error values resulting from a hierarchical structure that combines a mesotrophic monomictic with an eutrophic dimictic system. These results are not surprising as it would seem counterintuitive to improve ecological forecasts by exchanging information between systems that have substantial functional and structural differences. This numerical experiment merely aimed to provide an additional sensitivity analysis with regards to the role of the different parameters in accommodating the variability of the two datasets.

4.3. Outstanding methodological issues and future perspectives

In conclusion, we introduced a Bayesian hierarchical framework that enables the development of robust probabilistic analysis of error and uncertainty in model predictions by explicitly taking into account the measurement error, parameter uncertainty, and model structure imperfection. Our intent was to illustrate how this approach can be used to transfer knowledge in space, and therefore to simultaneously calibrate process-based models at multiple sites. Some of the unresolved technical aspects and future perspectives of the Bayesian hierarchical scheme are as follows:

(i) *Hierarchical Bayes and spatially explicit mathematical models:* The description of spatial and spatiotemporal environmental processes has been the focus of several Bayesian modeling studies, and the existing propositions involve general hierarchical spatial model frameworks (Cressie, 2000; Wikle, 2003a), Markov random field models (Besag et al., 1995), hierarchical spatio-temporal models (Wikle et al., 1998), spatiotemporal dynamic models (Wikle et al., 2001), and spatiotemporal models that are simplified by dimension reduction (Berliner et al., 2000) or by conditioning on processes considered to be latent or hidden (Hughes and Guttorp, 1994). In the

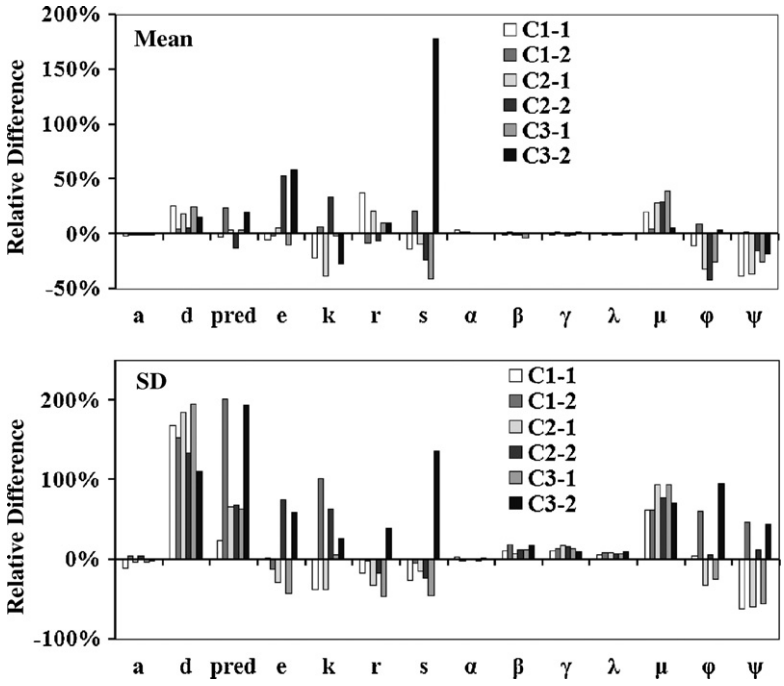

Fig. 9. *Scenario C.* The relative difference between posterior estimates of the mean values and standard deviations of the hyperparameters and the system-specific parameters. Relative difference$_k$ = (Parameter$_k$ − Global parameter)/Global parameter × 100%, k = submodel 1, 2.

present study, we advocated the relaxation of the assumption of globally common parameter values used in coupled physical-biogeochemical models and the adoption of hierarchical statistical formulations reflecting the more realistic notion that each site is unique but shares some commonality of behaviour with other sites of the same system. The proposed hierarchical structure will be easily employed with model segmentations of 5–10 completely mixed boxes without significant increase of the computation demands, while future research should also evaluate formulations that explicitly consider the spatiotemporal dependence patterns of the parameter values and model error terms.

(ii) *Mathematical models fitted to cross-system data:* In aquatic ecosystem modeling, cross-system data have been used in a global sense to develop empirical relationships between catchment features and nutrient loading (Howarth et al., 1996), lake morphometric/hydraulic characteristics and total phosphorus concentrations (Brett and Benjamin, 2008), light/nutrient availability and phytoplankton levels (Smith, 1986; Malve and Qian, 2006), algal and zooplankton biomass (McCauley and Kalff, 1981). In this context, the proposed framework is a logical advancement that allows developing models with stronger mechanistic foundation while remaining within the bounds of data-based parameter estimation (Borsuk et al., 2001). The main advantage of such hierarchical model configuration will be the effective modeling of systems with limited information by borrowing strength from well-studied systems. Indeed, our analysis showed that this approach provides ecologically meaningful parameter estimates at locations with limited data as well as site-specific predictions with more realistic uncertainty ranges than the conventional pooled approaches. Future research should identify the most appropriate criteria (trophic status, morphological characteristics) for delineating the number of levels and type of groups included in the hierarchical structures, thereby optimizing the transfer of information across systems, e.g., see the geomorphological typology presented in Malve and Qian (2006).

(iii) *Prior assumptions on parameter distributions and model structure:* The prior distributions assigned to the hyperparameters of hierarchical models have received considerable attention in the Bayesian literature (Box and Tiao, 1973; Spiegelhalter et al., 2003; Gelman et al., 1995), and special emphasis has been placed on the use of appropriate noninformative priors for hierarchical variance parameters (Gelman, 2005). In the context of the present analysis, we also caution to carefully select the priors for the error terms representing the discrepancy between the model structure and the natural system dynamics, as our experience was that some of the results presented herein were sensitive to the pertinent selection. We also note the instrumental role of the parameters associated with the zooplankton feeding kinetics and the mortality/higher predation rates in accommodating the site-specific variability. In this regard, an appealing next step would be the development of a prescriptive approach for optimizing the structure of hierarchical modeling constructs by choosing site specific closure terms (linear, quadratic, hyperbolic, sigmoid) or functional forms for zooplankton grazing (linear, saturating, saturating with feeding threshold, acclimating to ambient food) on the basis of the posterior parameter and model output patterns.

Acknowledgments

Funding for this study was provided by the National Sciences and Engineering Research Council of Canada (NSERC, Discovery Grants), the Connaught Committee (University of Toronto, Matching Grants 2006–2007), and the Ontario Graduate Scholarships (Ontario Ministry of Training, Colleges and Universities). All the material pertinent to this study is available upon request from the second author.

Appendix A.

Tables A1, A2, A3, A4 and A5.

Table A1
The specific functional forms of the aquatic biogeochemical model.

$$\frac{d\mathrm{PO_4}}{dt} = -\frac{\mathrm{PO_4}}{e+\mathrm{PO_4}}a\sigma_{(t)}\mathrm{PHYT}\,P/C_{\mathrm{phyto}} + \frac{\beta\lambda((\mathrm{PHYT}\cdot P/C_{\mathrm{phyto}})^2+\omega\mathrm{DET}^2)}{\mu^2+(\mathrm{PHYT}\cdot P/C_{\mathrm{phyto}})^2+\omega\mathrm{DET}^2}\sigma_{(tz)}\mathrm{ZOOP}\,P/C_{\mathrm{zoop}} + \gamma d\sigma_{(tz)}\frac{\mathrm{ZOOP}^3}{\mathrm{pred}^2+\mathrm{ZOOP}^2}P/C_{\mathrm{zoo}} + \phi\sigma_{(t)}\mathrm{DET} + k(1-\sigma_{(t)})(\mathrm{PO_{4(hypo)}}-\mathrm{PO_4}) + \mathrm{PO_{4exog}} - \mathrm{outflows}\cdot\mathrm{PO_4}$$

$$\frac{d\mathrm{PHYT}}{dt} = \frac{\mathrm{PO_4}}{e+\mathrm{PO_4}}a\sigma_{(t)}\mathrm{PHYT} - r\sigma_{(t)}\mathrm{PHYT} - \frac{\lambda(\mathrm{PHYT}\cdot P/C_{\mathrm{phyto}})^2}{\mu^2+(\mathrm{PHYT}\cdot P/C_{\mathrm{phyto}})^2+\omega\mathrm{DET}^2}\sigma_{(tz)}\mathrm{ZOOP} - s\mathrm{PHYT} - \mathrm{outflows}\cdot\mathrm{PHYT}$$

$$\frac{d\mathrm{ZOOP}}{dt} = \frac{\alpha\lambda((\mathrm{PHYT}\cdot P/C_{\mathrm{phyto}})^2+\omega\mathrm{DET}^2)}{\mu^2+(\mathrm{PHYT}\cdot P/C_{\mathrm{phyto}})^2+\omega\mathrm{DET}^2}\sigma_{(tz)}\mathrm{ZOOP} - d\sigma_{(tz)}\frac{\mathrm{ZOOP}^3}{\mathrm{pred}^2+\mathrm{ZOOP}^2} - \mathrm{outflows}\cdot\mathrm{ZOOP}$$

$$\frac{d\mathrm{DET}}{dt} = r\sigma_{(t)}\mathrm{PHYT}\,P/C_{\mathrm{phyto}} + \frac{[(1-\alpha-\beta)(\mathrm{PHYT}\cdot P/C_{\mathrm{phyto}})^2-(\alpha+\beta)\omega\mathrm{DET}^2]\lambda}{\mu^2+(\mathrm{PHYT}\cdot P/C_{\mathrm{phyto}})^2+\omega\mathrm{DET}^2}\sigma_{(tz)}\mathrm{ZOOP}\,P/C_{\mathrm{zoop}} - \varphi\,\sigma_{(t)}\mathrm{DET} - \psi\mathrm{DET} + \mathrm{DET_{exog}} - \mathrm{outflows}\cdot\mathrm{DET}$$

P/C_{phyto} (phosphorus to carbon ratio for phytoplankton): 0.015 mg P (mg C)$^{-1}$; P/C_{zoop} (phosphorus to carbon ratio for zooplankton): 0.029 mg P (mg C)$^{-1}$; ω (relative zooplankton preference for detritus compared to phytoplankton): 1; $\sigma_{(t)}$ and $\sigma_{(tz)}$: seasonal forcing on phytoplankton and zooplankton dynamics (Arhonditsis et al., 2008b); $\mathrm{PO_{4exog}}$, $\mathrm{DET_{exog}}$,: phosphate and particulate matter inflows into the system (Arhonditsis et al., 2008b); *Outflows:* outflows from the system (Arhonditsis et al., 2008b).

Table A2
Markov Chain Monte Carlo posterior estimates of the mean values and standard deviations of the model stochastic nodes against three datasets representing oligo-, meso-, and eutrophic conditions.

Nodes	Oligotrophic		Mesotrophic		Eutrophic	
	Mean	S. D.	Mean	S. D.	Mean	S. D.
a	1.129	0.130	1.273	0.189	1.073	0.058
d	0.182	0.024	0.183	0.022	0.188	0.020
pred	45.04	10.98	53.68	10.50	66.75	15.61
e	5.749	0.947	13.17	3.336	22.05	2.928
k	0.008	0.001	0.028	0.006	0.029	0.006
r	0.174	0.035	0.180	0.031	0.090	0.009
s	0.043	0.012	0.028	0.011	0.044	0.008
α	0.481	0.182	0.469	0.132	0.560	0.079
β	0.256	0.088	0.256	0.088	0.224	0.073
γ	0.287	0.106	0.297	0.113	0.275	0.064
λ	0.659	0.113	0.641	0.110	0.686	0.077
μ	6.597	1.724	7.280	1.624	8.577	1.362
φ	0.051	0.015	0.073	0.021	0.088	0.018
ψ	0.045	0.028	0.055	0.020	0.101	0.023
$\sigma_{\mathrm{PO_4}}$	5.272	0.487	14.43	1.661	27.51	2.464
σ_{PHYT}	38.59	4.383	69.35	8.032	131.5	14.86
σ_{ZOOP}	9.750	1.449	20.02	3.824	36.42	4.822
σ_{DET}	7.657	0.968	19.05	3.677	36.68	5.324

Table A3
Scenario A. Markov Chain Monte Carlo posterior estimates of the mean values and standard deviations of the model stochastic nodes.

Nodes	A_1				A_2			
	1		2		1		2	
	Mean	S. D.	Mean	S. D.	Mean	S. D.	Mean	S. D.
a	1.472	0.168	1.525	0.216	1.172	0.123	1.159	0.114
d	0.215	0.060	0.199	0.053	0.257	0.067	0.282	0.056
pred	55.08	22.36	46.93	28.35	56.13	15.29	101.6	28.14
e	17.65	2.535	12.30	2.230	13.17	1.997	25.92	6.161
k	0.020	0.007	0.005	0.001	0.019	0.004	0.023	0.006
r	0.174	0.034	0.152	0.022	0.187	0.016	0.179	0.039
s	0.026	0.012	0.022	0.007	0.016	0.008	0.018	0.012
α	0.523	0.198	0.522	0.197	0.673	0.130	0.685	0.119
β	0.229	0.089	0.236	0.094	0.247	0.094	0.241	0.083
γ	0.303	0.104	0.307	0.109	0.233	0.077	0.229	0.076
λ	0.626	0.124	0.627	0.123	0.722	0.123	0.724	0.119
μ	12.60	4.276	9.703	2.952	13.17	3.565	16.22	5.416
φ	0.038	0.019	0.028	0.011	0.039	0.009	0.054	0.025
ψ	0.027	0.007	0.030	0.006	0.031	0.007	0.042	0.015
$\sigma_{\mathrm{PO_4}}$	14.50	1.241	5.689	0.514	14.44	1.283	28.21	2.283
σ_{PHYT}	65.90	7.411	35.11	3.685	66.34	6.500	119.4	13.00
σ_{ZOOP}	19.58	2.933	9.557	1.473	19.48	2.785	34.82	4.860
σ_{DET}	16.39	2.238	7.329	0.936	17.17	2.136	35.66	4.810

Table A4
Scenario B. Markov Chain Monte Carlo posterior estimates of the mean values and standard deviations of the model stochastic nodes.

Nodes	B_1			
	1		2	
	Mean	S. D.	Mean	S. D.
a	1.303	0.092	1.317	0.087
d	0.288	0.066	0.263	0.058
pred	53.42	14.07	57.12	15.21
e	13.66	2.278	11.61	2.129
k	0.028	0.006	0.039	0.006
r	0.153	0.033	0.134	0.032
s	0.032	0.011	0.046	0.012
α	0.772	0.126	0.779	0.121
β	0.215	0.078	0.218	0.082
γ	0.232	0.069	0.240	0.062
λ	0.738	0.103	0.739	0.105
μ	8.753	2.863	7.611	2.244
φ	0.072	0.030	0.064	0.023
ψ	0.044	0.017	0.046	0.015
$\sigma_{\mathrm{PO_4}}$	14.51	1.344	14.63	1.591
σ_{PHYT}	67.48	6.779	60.50	6.799
σ_{ZOOP}	18.49	2.601	17.24	2.373
σ_{DET}	18.16	2.352	17.21	2.416

Table A5
Scenario D. Markov Chain Monte Carlo posterior estimates of the mean values and standard deviations of the model stochastic nodes.

Nodes	D_1				D_2			
	1		2		1		2	
	Mean	S. D.	Mean	S. D.	Mean	S. D.	Mean	S. D.
a	1.316	0.217	1.399	0.159	1.028	0.096	1.027	0.116
d	0.458	0.143	0.317	0.154	0.417	0.128	0.379	0.101
pred	69.63	20.83	44.64	59.81	68.12	19.87	136.2	36.62
e	15.70	4.812	12.03	2.552	11.31	2.052	23.61	9.309
k	0.020	0.006	0.004	0.001	0.019	0.004	0.022	0.006
r	0.170	0.055	0.151	0.027	0.176	0.025	0.172	0.074
s	0.019	0.012	0.013	0.008	0.015	0.010	0.018	0.008
α	0.740	0.155	0.673	0.235	0.746	0.142	0.772	0.099
β	0.225	0.125	0.252	0.178	0.186	0.094	0.177	0.099
γ	0.216	0.118	0.336	0.209	0.294	0.102	0.247	0.095
λ	0.823	0.127	0.796	0.149	0.783	0.124	0.799	0.114
μ	9.783	4.563	9.280	3.407	13.730	3.508	18.55	9.417
φ	0.076	0.062	0.020	0.012	0.029	0.014	0.063	0.031
ψ	0.041	0.025	0.022	0.006	0.026	0.007	0.066	0.061
$\sigma_{\mathrm{PO_4}}$	14.13	1.367	5.837	0.548	14.98	1.344	28.74	2.622
σ_{PHYT}	64.30	6.766	34.65	3.697	67.83	6.561	124.8	14.39
σ_{ZOOP}	18.34	2.709	9.243	1.468	19.16	2.798	32.86	4.499
σ_{DET}	16.94	2.241	6.971	0.795	16.44	2.068	35.14	4.986

References

Arhonditsis, G.B., Brett, M.T., Frodge, J., 2003. Environmental control and limnological impacts of a large recurrent spring bloom in Lake Washington, USA. Environ. Manage. 31 (5), 603–618.

Arhonditsis, G.B., Brett, M.T., 2004. Evaluation of the current state of mechanistic aquatic biogeochemical modeling. Mar. Ecol. Prog. Ser. 271, 13–26.

Arhonditsis, G.B., Adams-VanHarn, B.A., Nielsen, L., Stow, C.A., Reckhow, K.H., 2006. Evaluation of the current state of mechanistic aquatic biogeochemical modeling: citation analysis and future perspectives. Environ. Sci. Technol. 40 (21), 6547–6554.

Arhonditsis, G.B., Qian, S.S., Stow, C.A., Lamon, E.C., Reckhow, K.H., 2007. Eutrophication risk assessment using Bayesian calibration of process-based models: application to a mesotrophic lake. Ecol. Model. 208 (2–4), 215–229.

Arhonditsis, G.B., Papantou, D., Zhang, W., Perhar, G., Massos, E., Shi, M., 2008a. Bayesian calibration of mechanistic aquatic biogeochemical models and benefits for environmental management. J. Mar. Syst. 73, 8–30.

Arhonditsis, G.B., Perhar, G., Zhang, W., Massos, E., Shi, M., Das, A., 2008b. Addressing equifinality and uncertainty in eutrophication models. Water Resour. Res. 44, W01420.

Berliner, L.M., 1996. In: Hanson, K., Silver, R. (Eds.), Hierarchical Bayesian Time Series Models. Maximum Entropy and Bayesian Methods. Kluwer, Norwell, pp. 15–22.

Berliner, L.M., Wikle, C.K., Cressie, N., 2000. Long-lead prediction of Pacific SSTs via Bayesian dynamic modeling. J. Climate 13 (22), 3953–3968.

Bernardo, J.M., Smith, A.F.M., 1994. Bayesian Theory. John Wiley & Sons, New York.

Besag, J., Green, P., Higdon, D., Mengersen, K., 1995. Bayesian computation and stochastic systems. Stat. Sci. 10 (1), 3–66.

Beven, K.J., 2001. Rainfall-Runoff Modeling: The Primer. John Wiley & Sons, New York.

Borsuk, M.E., Higdon, D., Stow, C.A., Reckhow, K.H., 2001. A Bayesian hierarchical model to predict benthic oxygen demand from organic matter loading in estuaries and coastal zones. Ecol. Model. 143 (3), 165–181.

Box, G.E.P., Tiao, G.C., 1973. Bayesian Inference in Statistical Analysis. Addison-Wesley, Reading.

Brett, M.T., Benjamin, M.M., 2008. A review and reassessment of lake phosphorus retention and the nutrient loading concept. Freshwater Biol. 53 (1), 194–211.

Brooks, S.P., Gelman, A., 1998. Alternative methods for monitoring convergence of iterative simulations. J. Comput. Graph. Stat. 7 (4), 434–455.

Brun, R., Reichert, P., Kunsch, H.R., 2001. Practical identifiability analysis of large environmental simulation models. Water Resour. Res. 37 (4), 1015–1030.

Chapra, S.C., Canale, R.P., 1998. Numerical Methods for Engineers, 3rd ed. McGraw-Hill, New York.

Chen, C.F., Ma, H.W., Reckhow, K.H., 2007. Assessment of water quality management with a systematic qualitative uncertainty analysis. Sci. Total Environ. 374 (1), 13–25.

Clark, J.S., 2003. Uncertainty in population growth rates calculated from demography: the hierarchical approach. Ecology 84 (6), 1370–1381.

Clark, J.S., 2005. Why environmental scientists are becoming Bayesians. Ecol. Lett. 8 (1), 2–14.

Clark, J.S., Dietze, M., Chakraborty, S., Agarwal, P.K., Ibanez, I., LaDeau, S., Wolosin, M., 2007. Resolving the biodiversity paradox. Ecol. Lett. 10 (8), 647–659.

Cressie, N., 2000. Spatial statistics and environmental sciences. In: Proceedings of the Section on Statistics and the Environment. American Statistical Association, Alexandria, pp. 1–10.

Dennis, B., 1996. Discussion: should ecologists become Bayesians? Ecol. Appl. 6 (4), 1095–1103.

Dorazio, R.M., Johnson, F.A., 2003. Bayesian inference and decision theory—a framework for decision making in natural resource management. Ecol. Appl. 13 (2), 556–563.

Edwards, A.M., Yool, A., 2000. The role of higher predation in plankton population models. J. Plankton Res. 22 (6), 1085–1112.

Efron, B., Morris, C.N., 1975. Data analysis using Stein's estimator and its generalizations. J. Am. Stat. Assoc. 70 (350), 311–319.

Ellison, A.M., 1996. An introduction to Bayesian inference for ecological research and environmental decision-making. Ecol. Appl. 6 (4), 1036–1046.

Ellison, A.M., 2004. Bayesian inference in ecology. Ecol. Lett. 7 (6), 509–520.

Endres, D.M., Schindelin, J.E., 2003. A new metric for probability distributions. IEEE T. Inform. Theory 49 (7), 1858–1860.

Engeland, K., Gottschalk, L., 2002. Bayesian estimation of parameters in a regional hydrological model. Hydrol. Earth Syst. Sci. 6, 883–898.

Franks, S.W., Gineste, P., Beven, K.J., Merot, P., 1998. On constraining the predictions of a distributed models: The incorporation of fuzzy estimates of saturated areas into the calibration process. Water Resour. Res. 34, 787–797.

Franks, P.J.S., 2002. NPZ models of plankton dynamics: their construction, coupling to physics, and application. J. Oceanogr. 58, 379–387.

Gelman, A., 2005. Analysis of variance—why it is more important than ever. Ann. Stat. 33 (1), 1–31.

Gelman, A., Pardoe, L., 2006. Bayesian measures of explained variance and pooling in multilevel (hierarchical) models. Technometrics 48 (2), 241–251.

Gelman, A., Carlin, J.B., Stern, H.S., Rubin, D.B., 1995. Bayesian Data Analysis. Chapman and Hall, New York.

Hampton, S.E., 2005. Increased niche differentiation between two *Conochilus* species over 33 years of climate change and food web alteration. Limnol. Oceanogr. 50 (2), 421–426.

Hong, B.G., Strawderman, R.L., Swaney, D.P., Weinstein, D.A., 2005. Bayesian estimation of input parameters of a nitrogen cycle model applied to a forested reference watershed Hubbard Brook Watershed Six. Water Resour. Res. 41 (3), W03007.

Howarth, R.W., Billen, G., Swaney, D., Townsend, A., Jaworski, N., Lajtha, K., Downing, J.A., Elmgren, R., Caraco, N., Jordan, T., Berendse, F., Freney, J., Kudeyarov, V., Murdoch, P., Zhu, Z., 1996. Regional nitrogen budgets and riverine N&P fluxes for the drainage to the North Atlantic Ocean: natural and human influences. Biogeochemistry 35 (1), 75–139.

Hughes, J.P., Guttorp, P., 1994. Incorporating spatial dependence and atmospheric data in a model of precipitation. J. Appl. Meteorol. 33 (12), 1503–1515.

Legendre, P., Legendre, L., 1998. Numerical Ecology, 2nd ed. Elsevier Science BV, Amsterdam.

Malve, O., Qian, S.S., 2006. Estimating nutrients and chlorophyll a relationships in Finnish lakes. Environ. Sci. Technol. 40 (24), 7848–7853.

Malve, O., Laine, M., Haario, H., 2005. Estimation of winter respiration rates and prediction of oxygen regime in a lake using Bayesian inference. Ecol. Model. 182 (2), 183–197.

Malve, O., Laine, M., Haario, H., Kirkkala, T., Sarvala, J., 2007. Bayesian modelling of algal mass occurrences—using adaptive MCMC methods with a lake water quality model. Environ. Modell. Softw. 22 (7), 966–977.

McCauley, E., Kalff, J., 1981. Empirical relationships between phytoplankton and zooplankton biomass in lakes. Can. J. Fish. Aquat. Sci. 38 (1), 458–463.

Neal, R., 1998. Suppressing random walks in Markov chain Monte Carlo using ordered over-relaxation. In: Jordan, M.I. (Ed.), Learning in Graphical Models. Kluwer Academic Publishers, Dordrecht, pp. 205–230.

Nicholls, K.H., 1999. Effects of temperature and other factors on summer phosphorus in the inner Bay of Quinte Lake Ontario: implications for climate warming. J. Great Lakes Res. 25 (2), 250–262.

Omlin, M., Reichert, P., 1999. A comparison of techniques for the estimation of model prediction uncertainty. Ecol. Model. 115 (1), 45–59.

Page, T., Beven, K.J., Whyatt, J.D., 2004. Predictive capability in estimating changes in water quality: long-term responses to atmospheric deposition. Water Air Soil Pollut. 151 (1–4), 215–244.

Qian, S.S., Stow, C.A., Borsuk, M.E., 2003. On Monte Carlo methods for Bayesian inference. Ecol. Model. 159 (2–3), 269–277.

Qian, S.S., Reckhow, K.H., 2007. Combining model results and monitoring data for water quality assessment. Environ. Sci. Technol. 41 (14), 5008–5013.

Reichert, P., Omlin, M., 1997. On the usefulness of overparameterized ecological models. Ecol. Model. 95 (2–3), 289–299.

Reichert, P., Schervish, M., Small, M.J., 2002. An efficient sampling technique for Bayesian inference with computationally demanding models. Technometrics 44 (4), 318–327.

Rockwell, D.C., Warren, G.J., Bertram, P.E., Salisbury, D.K., Burns, N.M., 2005. The US EPA Lake Erie indicators monitoring program 1983–2002: trends in phosphorus, silica, and chlorophyll a in the central basin. J. Great Lakes Res. 31 (Suppl. 2), 23–34.

Royle, J.A., Berliner, L.M., Wikle, C.K., Milliff, R., 1999. A hierarchical spatial model for constructing wind fields from scatterometer data in the Labrador Sea. In: Gatsonis, C., et al. (Eds.), Case Studies in Bayesian Statistics. Springer-Verlag, pp. 367–382.

Schindler, D.W., 1997. Widespread effects of climatic warming on freshwater ecosystems in North America. Hydrol. Process. 11 (8), 1043–1067.

Schindler, D.W., 2001. The cumulative effects of climate warming and other human stresses on Canadian freshwaters in the new millennium. Can. J. Fish. Aquat. Sci. 58 (1), 18–29.

Smith, V.H., 1986. Light and nutrient effects on the relative biomass of blue-green algae in lake phytoplankton. Can. J. Fish. Aquat. Sci. 43 (1), 148–153.

Spiegelhalter, D., Thomas, A., Best, N., Lunn, D. 2003. WinBUGS User Manual, Version 1.4. (Available at http://www.mrc-bsu.cam.ac.uk/bugs).

Steinberg, L.J., Reckhow, K.H., Wolpert, R.L., 1997. Characterization of parameters in mechanistic models: a case study of a PCB fate and transport model. Ecol. Model. 97 (1–2), 35–46.

Stow, C.A., Reckhow, K.H., Qian, S.S., Lamon, E.C., Arhonditsis, G.B., Borsuk, M.E., Seo, D., 2007. Approaches to evaluate water quality model parameter uncertainty for adaptive TMDL implementation. J. Am. Water Resour. As. 43 (6), 1499–1507.

Straile, D., 2002. North Atlantic Oscillation synchronizes food-web interactions in central European lakes. P. Roy. Soc. Lond. B. Biol. 269 (1489), 391–395.

Thomas, C.D., Bodsworth, E.J., Wilson, R.J., Simmons, A.D., Davies, Z.G., Musche, M., Conradt, L., 2001. Ecological and evolutionary processes at expanding range margins. Nature 411 (6837), 577–581.

Weyhenmeyer, G.A., 2004. Synchrony in relationships between the North Atlantic Oscillation and water chemistry among Sweden's largest lakes. Limnol. Oceanogr. 49 (4), 1191–1201.

Wikle, C.K., 2003a. Hierarchical models in environmental science. Int. Stat. Rev. 71 (2), 181–199.

Wikle, C.K., 2003b. Hierarchical Bayesian models for predicting the spread of ecological processes. Ecology 84 (6), 1382–1394.

Wikle, C.K., Berliner, L.M., Cressie, N., 1998. Hierarchical Bayesian space-time models. J. Envir. Ecol. Stat. 5 (2), 117–154.

Wikle, C.K., Milliff, R.F., Nychka, D., Berliner, L.M., 2001. Spatiotemporal hierarchical Bayesian modeling: Tropical ocean surface winds. J. Am. Stat. Assoc. 96 (454), 382–397.

Wikle, C.K., Berliner, L.M., Milliff, R.F., 2003. Hierarchical Bayesian approach to boundary value problems with stochastic boundary conditions. Mon. Weather. Rev. 131 (6), 1051–1062.
Winter, J.G., Eimers, M.C., Dillon, P.J., Scott, L.D., Scheider, W.A., Willox, C.C., 2007. Phosphorus inputs to Lake Simcoe from 1990 to 2003: declines in tributary loads and observations on lake water quality. J. Great Lakes Res. 33 (2), 381–396.
Zhang, W., Arhonditsis, G.B., 2008. Predicting the frequency of water quality standard violations using Bayesian calibration of eutrophication models. J. Great Lakes Res. 34, 698–720.